Pergamon

0301-9322(95)00053-4

EFFECT OF GAS-PHASE THERMAL EXPANSION ON STABILITY OF DEFLAGRATIONS IN POROUS ENERGETIC MATERIALS

S. B. MARGOLIS[1] and F. A. WILLIAMS[2]

[1]Combustion Research Facility, Sandia National Laboratories, Livermore, CA 94551-0969, U.S.A.

[2]Department of Applied Mechanics and Engineering Sciences, University of California, San Diego, La Jolla, CA 92093-0310, U.S.A.

Abstract—Deflagration waves propagating through porous energetic materials are known to be subject to intrinsic diffusional/thermal instabilities that are associated with the onset of various oscillatory modes of combustion. A few theoretical analyses to explain these combustion phenomena have been published in the literature, and the present contribution extends these results. In particular, we reconsider our previous asymptotic analysis of non-steady, non-planar deflagration, which postulated a constant-density gas phase, to take into account the effects of quasi-steady thermal expansion of an ideal gas. With relative motion between gaseous and condensed phases included, a time-dependent, multidimensional asymptotic model is derived through the application of activation-energy asymptotics. Analyzing this model, an explicit solution corresponding to steady, planar deflagration is obtained as a special case, and a dispersion relation is derived describing its linear stability. In the plane defined by the non-dimensional activation energy and the disturbance wavenumber, a pulsating neutral stability boundary is calculated, beyond which non-steady, non-planar solutions are expected. The effects of porosity and gas-phase thermal expansion are shown to be generally destabilizing, suggesting that degraded propellants, which exhibit greater porosity than the pristine material, may be more readily subject to combustion instability and non-steady deflagration.

Key Words: porous energetic materials, deflagration, instability, activation-energy asymptotics

1. INTRODUCTION

There is increasing concern about the safety and surety of aging or thermally damaged propellants, explosives and pyrotechnic materials. This concern, in turn, has fostered an important and rapidly growing area of research focused on the combustion behavior of porous energetic solids. Interests include determining the ignition characteristics of such materials and the conditions under which low-speed deflagrations propagating in the materials can become unstable and undergo transition to detonation. The present contribution addresses the question of deflagration stability for one particular model in which an initially porous solid melts and subsequently undergoes a one-step Arrhenius combustion process in the liquid phase, producing heat and gaseous reaction products. This model is designed to provide a simplified description of the combustion of a class of energetic materials that includes some types of nitramine propellants, such as HMX, that are observed to exhibit considerable bubbling in an exothermic foam region during deflagration. In fact, multiphase combustion layers occur at the surfaces of most burning propellants, even those that initially are purely homogeneous solids. Thus, it is clear that, in such applications, two-phase-flow effects play an important role even for non-porous materials. However, a non-zero initial porosity, whether present by design or as a consequence of prior exposure to abnormal thermal environments, can clearly enhance the importance of two-phase flow with respect to deflagration and its stability, affecting not only fundamental thermodynamic characteristics such as the burned temperature, but also resulting in a more pronounced two-phase effect in the surface layer. This study takes a further step towards quantifying the influences of multiphase flow on the stability of the combustion process.

The literature contains a number of general formulations for multiphase flow in the combustion of energetic materials (cf. Baer & Nunziato 1986). Simplifying approximations may then be introduced into these formulations in order to describe particular combustion processes of interest. Early research on multiphase deflagration tended to treat two-phase flow as a one-phase process

through an appropriate averaging over the multiphase medium. Our previous works (Margolis et al. 1987; Li et al. 1990; Margolis & Williams 1990, 1995a, b) have shown that this type of approximation often conceals important effects of two-phase flow, such as influences of velocity and temperature differences between the two phases on the propagation velocity of the deflagration and its stability. The present paper, which is also based on a model that takes into account the different properties and velocities of the different phases, continues our investigation of the effects of two-phase flow on various aspects of propellant deflagration.

The simplified chemistry, consisting of a one-step exothermic process in which condensed (liquid) reactants are converted into gaseous products, of the present work is the same as that of all of our previous studies except one (Li et al. 1990), which added a reversible vaporization step and an irreversible gas-phase exothermic step to provide a better approximation for nitramine deflagration. Indeed, there are low-pressure situations in which the gas-phase chemistry occurs at locations sufficiently remote from the regressing surface that it can be neglected. However, even when this is not true, analyses that retain only the exothermic gasification process are necessary first steps in understanding complex phenomena such as stability behavior in multiphase reactive media. Our initial studies (Margolis et al. 1987; Li et al. 1990; Margolis & Williams 1990) also limited their considerations to non-porous materials by placing the solid–liquid interface at a sufficiently remote location ahead of the deflagration front. Our first treatment of effects associated with initial porosity (Margolis & Williams 1995a), which was restricted to steady, planar deflagration, demonstrated several important modifications relative to the non-porous case. For example, it was shown that the final burned temperature decreases as the porosity increases because of the energy required to heat the gas contained in the pores, thereby substantially reducing the burning rate, which depends exponentially on the final burned temperature. Our latest publication on the subject (Margolis & Williams 1995b), which differs from the present work in that the gas density was assumed constant, adopted the same generic model but generalized the analysis to address the non-steady, non-planar stability of the steady, planar solution under the same assumption of constant gas density. That analysis was thus similar to our previous analysis of the non-porous case (Margolis & Williams 1990), which is now seen to correspond to the non-porous limit of the more recent study. The present work, in contrast, retains variable-density effects associated with the thermal expansion of the gas. To facilitate the analysis, a quasi-steady approximation is applied to the gas phase and, analogous to our earlier work on deflagration stability described above, the method of activation-energy asymptotics is employed to derive a non-steady, multidimensional asymptotic model, a basic solution corresponding to steady, planar deflagration, and a dispersion relation governing its linear stability.

2. DISCUSSION AND FORMULATION

Figure 1 is a schematic diagram of the propagating deflagration wave, which moves generally to the left into the porous unburned solid that has a gas-phase volume fraction ϵ_s. The structure of the combustion wave, which, we emphasize, may propagate in a non-steady and non-planar fashion is as follows. Proceeding from left to right, there exists a solid–gas preheat region, a melting front at which the solid constituent becomes liquid upon reaching its melting temperature $\tilde{T}_m$ and a further region of liquid–gas heating that completes region (1) in figure 1. This is followed by a relatively thin exothermic reaction zone, identified as region (2) in figure 1, where the liquid reacts to form gaseous products. This in turn is followed by the burnt-gas region (3), where the volume fraction ϵ of the gas is unity. In the limit that the activation energy of reaction is large, the reaction zone (2) asymptotically becomes a propagating surface similar to, but displaced from, the melting surface. In the laboratory-fixed spatial coordinate system $(\tilde{x}_1, \tilde{x}_2, \tilde{x}_3)$ illustrated in figure 1, the porous solid extends to $\tilde{x}_3 = -\infty$, where conditions are denoted by the subscript u, and the gas extends to $\tilde{x}_3 = +\infty$, where conditions are identified by the subscript b. The deflagration generally propagates in the $-\tilde{x}_3$ direction, although, as noted above, the wave motion is allowed to be both non-steady and non-planar. Here and in what follows, a tilde over a symbol (e.g. $\tilde{x}_3$) will denote a dimensional quantity, and the subscripts s, L and G will denote solid, liquid and gas-phase quantities, respectively. A continuum formulation, in which appropriate volume fractions multiply

the physical variables associated with each phase, will be used to model the physical problem just described.

The formulation of the problem may be presented either by beginning with a very general mathematical description, and then introducing many simplifying assumptions, or by stating approximations physically and then immediately writing down the mathematical formulation to be used. The first of these two approaches has the advantage of exhibiting explicitly many of the approximations that are adopted, but has the disadvantage of being lengthy and tending to divert attention to relatively unimportant side issues. Because of this disadvantage, and because the initial formulation has been formally presented in our previous work (Margolis & Williams 1995a, b), we have adhered more closely to the second approach in the present study. Specifically, the formulation for planar problems in which the solutions do not depend on the transverse co-ordinates $\tilde{x}_2$ and $\tilde{x}_3$ was given in Margolis & Williams (1995a), and generalized in Margolis & Williams (1995b) to weakly non-planar deflagrations in which the product of the amplitude and the transverse wavenumber of the non-planar disturbance is small. This is an appropriate regime for analyzing the stability of planar solutions of the system, and permits considerable simplification in the representation of the velocity field. In particular, the transverse velocity components in the $\tilde{x}_1$- and $\tilde{x}_2$-directions are small compared with the component in the $\tilde{x}_3$-direction, and can be neglected to the order of approximation needed here. That is, the velocity $\tilde{u}$ in each phase may be approximated by $\tilde{u}_{L,G} = (0, 0, \tilde{u}_{L,G}(\tilde{x}_1, \tilde{x}_2, \tilde{x}_3, \tilde{t}))$, where the velocity of the solid phase is assumed to be zero. A considerable number of simplifications then occur in all of the conservation equations, and ultimately the primary differences that remain between the formulations for the planar and non-planar problems are the presence in the latter of additional terms involving transverse derivatives that arise from transverse diffusion. It is noteworthy that non-planar stability can be addressed through a formulation that resembles so closely the formulation for time-dependent, planar combustion.

In addition to the velocities, the formulations in our aforementioned previous studies allow for the temperatures of the gaseous and condensed phases to differ from one another as well, as they must when convective enthalpy transport by the gas phase relative to the condensed phase is important (cf. Aldushin 1990; Aldushin & Zeinenko 1991). They also account, in an approximate way, for influences and of viscous and surface-tension-gradient forces on velocities, following an earlier analysis (Margolis et al. 1987) of steady, planar deflagration in non-porous propellants. These effects have been included in a stability analysis for such propellants assuming constant gas-phase density (Margolis & Williams 1990), where it was found that surface-tension-gradient
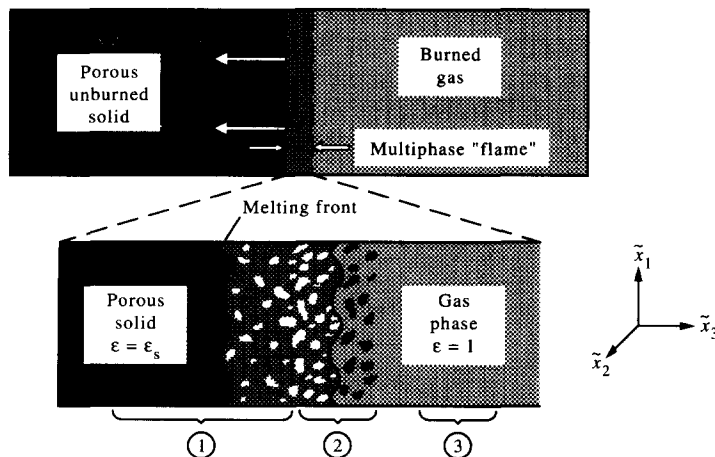

Figure 1.q Non-steady deflagration of a porous energetic material with two-phase flow in both the solid–gas and liquid–gas regions, with combustion occurring in the latter. The lower figure is a blow-up of the multiphase, multidimensional "flame" structure, consisting minimally of (1) a preheat zone containing a time-dependent, non-planar melting front, specified functionally by $\tilde{x}_3 = \tilde{x}_m(\tilde{x}_1, \tilde{x}_2, \tilde{t})$, across which the porous solid changes into a bubbly liquid, or foam, and (2) a thin liquid–gas reaction zone. Additional gas-phase reactions, suppressed in the present work, may occur in a secondary gas-flame region (3) downstream from the primary two-phase reaction zone (2).

forces and resistance to heat transmission are both destabilizing. Qualitatively, the same result may be expected for the porous propellants considered here. For simplicity, however, and because of uncertainties in values of surface tension and interphase heat-transfer coefficients, we neglected these effects in our final analysis of the model given in Margolis & Williams (1995b). For the sake of economy, we shall exclude these effects at the outset in the present study, referring the reader to that earlier publication for the more general formulation.

In writing the resulting conservation equations for the single-temperature limit described above, the symbols $\tilde{\rho}$, $\tilde{u}$ and $\tilde{t}$ are used for density, the $\tilde{x}_3$-component of velocity and time, respectively, with appropriate subscripts identifying each phase. Denoting the location of the melting surface by $\tilde{x}_3 = \tilde{x}_m(\tilde{x}_1, \tilde{x}_2, t)$, we have, in the laboratory-fixed co-ordinate system and with the approximations described above,

$$\tilde{u}_s = 0, \quad \tilde{u}_L = -\frac{\partial \tilde{x}_m}{\partial \tilde{t}} \left(\frac{\tilde{\rho}_s}{\tilde{\rho}_L} - 1 \right), \qquad [1]$$

where $\tilde{\rho}_s$ and $\tilde{\rho}_L$ are both assumed to be known constants. These results, coupled with the small Mach-number assumption mentioned below, make it unnecessary to consider momentum conservation any further (Margolis et al. 1987) and thus enable us to focus attention on mass and energy conservation, which thus dominate the process analyzed here. In particular, denoting the gas-phase volume fraction by ϵ, overall mass conservation can be written as

$$\frac{\partial \tilde{\rho}_G}{\partial t} + \frac{\partial}{\partial \tilde{x}_3}(\tilde{\rho}_G \tilde{u}_G) = 0, \quad \tilde{x}_3 < \tilde{x}_m, \qquad [2]$$

and

$$\frac{\partial}{\partial \tilde{t}}[(1 - \epsilon)\tilde{\rho}_L + \epsilon \tilde{\rho}_G] + \frac{\partial}{\partial \tilde{x}_3}[(1 - \epsilon)\tilde{\rho}_L \tilde{u}_L + \epsilon \tilde{\rho}_G \tilde{u}_G] = 0, \quad \tilde{x}_3 > \tilde{x}_m. \qquad [3]$$

In addition, conservation of mass of the liquid phase is expressed as

$$\frac{\partial}{\partial \tilde{t}}[(1 - \epsilon)\tilde{\rho}_L] + \frac{\partial}{\partial \tilde{x}_3}[(1 - \epsilon)\tilde{\rho}_L \tilde{u}_L] = -\tilde{A}\tilde{\rho}_L(1 - \epsilon)\exp(-\tilde{E}/\tilde{R}°\tilde{T}), \quad \tilde{x}_3 > \tilde{x}_m, \qquad [4]$$

where $\tilde{T}$ denotes temperature, $\tilde{E}$ is the overall activation energy, $\tilde{R}°$ is the universal gas constant, and $\tilde{A}$ is the pre-exponential reciprocal-time factor (assumed constant here) for the rate of the overall exothermic chemical reaction by which the liquid is transformed to gaseous products. The statement of mass conservation for the gas in the region $\tilde{x}_3 > \tilde{x}_m$ is the difference between [3] and [4]. We note that in the solid–gas region $\tilde{x}_3 < \tilde{x}_m$, condensed continuity is identically satisfied since $\tilde{\rho}_s = \tilde{u}_s = 0$, and assuming initially constant porosity ϵ_s for the unburned material, $\epsilon = \epsilon_s$ throughout this region. As a result, the overall continuity equation [2] in the solid–gas region collapses to the continuity equation for the gas phase alone. In the liquid–gas region $\tilde{x}_3 > \tilde{x}_m$, ϵ varies according to [4] and approaches unity as combustion goes to completion. As discussed in Margolis et al. (1987), the evaluation of the Arrhenius reaction rate is based on conditions (e.g. temperature) in the liquid phase, and may be interpreted as a contribution to a constitutive relation for that medium.

The equation for overall energy conservation can be expressed as

$$\frac{\partial}{\partial \tilde{t}}\{[\tilde{\rho}_s \tilde{c}_s(1 - \epsilon_s) + \tilde{\rho}_G \tilde{c}_G \epsilon_s]\tilde{T}\} + \frac{\partial}{\partial \tilde{x}_3}(\tilde{\rho}_G \tilde{c}_G \tilde{u}_G \epsilon_s \tilde{T})$$

$$= \tilde{\nabla} \cdot \{[\tilde{\lambda}_s(1 - \epsilon_s) + \tilde{\lambda}_G \epsilon_s]\tilde{\nabla}\tilde{T}\} + \epsilon_s \frac{\partial \tilde{p}_G}{\partial t}, \quad \tilde{x}_3 < \tilde{x}_m, \quad [5]$$

and

$$\frac{\partial}{\partial \tilde{t}}[\tilde{\rho}_L(1 - \epsilon)(\tilde{Q} + \tilde{c}_L \tilde{T}) + \tilde{\rho}_G \tilde{c}_G \epsilon \tilde{T}] + \frac{\partial}{\partial \tilde{x}_3}(\tilde{\rho}_L \tilde{u}_L(1 - \epsilon)(\tilde{Q} + \tilde{c}_L \tilde{T}) + \tilde{\rho}_G \tilde{c}_G \tilde{u}_G \epsilon \tilde{T}]$$

$$= \tilde{\nabla} \cdot \{[\tilde{\lambda}_L(1 - \epsilon) + \tilde{\lambda}_G \epsilon]\tilde{\nabla}\tilde{T}\} + \epsilon \frac{\partial \tilde{p}_G}{\partial t}, \quad \tilde{x}_3 > \tilde{x}_m, \quad [6]$$

in the solid–gas and liquid–gas regions, respectively. Here, $\tilde{c}$, $\tilde{\lambda}$ and $\tilde{p}$ denote specific heats at constant pressure (assumed constant and, for condensed phases, equal to the corresponding specific heats at constant volume), thermal conductivities (also later treated as constants) and pressure, respectively. The heat released per unit mass in the chemical reaction is denoted by $\tilde{Q}$, which serves to define the chemical enthalpy difference between the gaseous and liquid phases, and which varies with $\tilde{T}$ unless $\tilde{c}_L = \tilde{c}_G$. Conservation of energy for the condensed phases can also be written down, but are not needed when the temperatures are the same in each co-existing phase. Equations for the gas phase may then be obtained by subtracting the appropriate condensed-phase equation from the corresponding overall energy equation. Derivations of alternative forms of these conservation equations for the more general two-temperature formulation is contained in our previous work (Margolis & Williams 1995a, b), where it is also shown how [5] and [6] are obtained as the appropriate limit in the limit of large rates of interphase heat transfer. Additional discussions are also given regarding the roles and origins of various terms. In particular, we remark that the term involving $\tilde{p}_G$, which, for small Mach numbers, depends at most on $\tilde{t}$, arises from the contributions of surface and volume work performed by the gas to the rate of change in its internal energy.

The (ideal) equation of state for the gas to be used in the present work is

$$\tilde{p}_G = \tilde{\rho}_G \tilde{R}^\circ \tilde{T} / \tilde{W}_G,\qquad [7]$$

where $\tilde{W}_G$ denotes the molecular weight of the gas. As indicated above, the Mach number is assumed to be small, under which condition $\tilde{p}_G$ is independent of the spatial coordinates (Margolis & Williams 1995a, b) and its partial derivative with respect to $\tilde{t}$ becomes a total derivative. Equation [7] thus takes into account compressibility of the gas, and since $\tilde{\rho}_s$ and $\tilde{\rho}_L$ are constants, this completes the set of equations, subject to boundary and interface conditions prescribed below, needed to describe a deflagration in the porous material. Boundary conditions appropriate for an unconfined deflagration are given by

$$\epsilon = \epsilon_s \quad \text{for} \quad \tilde{x}_3 < \tilde{x}_m; \quad \tilde{u}_G \to 0, \quad \tilde{T} \to \tilde{T}_u \quad \text{as} \quad \tilde{x} \to -\infty,\qquad [8]$$

$$\epsilon \to 1, \quad \tilde{p}_G \to \tilde{p}_G^\circ, \quad \tilde{T} \to \tilde{T}_b \quad \text{as} \quad \tilde{x}_3 \to +\infty,\qquad [9]$$

where the final burned temperature $\tilde{T}_b$ is determined from $\tilde{Q}$ and thermal properties of the system, and the boundary condition on pressure implies that $\tilde{p}_G = \tilde{p}_G^\circ$ everywhere. For the approximations adopted here, the interface conditions across the melting surface collapse to continuity of ϵ, $\tilde{u}_G$ and $\tilde{T}$ (Margolis & Williams 1995b), where

$$\epsilon|_{\tilde{x}_3 = \tilde{x}_m} = \epsilon_s, \quad \tilde{T}|_{\tilde{x}_3 = \tilde{x}_m} = \tilde{T}_m,\qquad [10]$$

and the overall interface energy balance

$$G_m\{[\tilde{\lambda}_L(1 - \epsilon_s) + \tilde{\lambda}_G \epsilon_s]\hat{n}_m \cdot \tilde{\nabla}\tilde{T}|_{\tilde{x}_3 = \tilde{x}_m^+} - [\tilde{\lambda}_s(1 - \epsilon_s) + \tilde{\lambda}_G \epsilon_s]\hat{n}_m \cdot \tilde{\nabla}\tilde{T}|_{\tilde{x}_3 = \tilde{x}_m^-}\}$$

$$= (1 - \epsilon_s)\left\{\tilde{\rho}_s \tilde{\gamma}_s \frac{\partial \tilde{x}_m}{\partial \tilde{t}} + \left[\tilde{\rho}_L \tilde{c}_L\left(\tilde{u}_L|_{\tilde{x}_3 = \tilde{x}_m^+} - \frac{\partial \tilde{x}_m}{\partial \tilde{t}}\right) - \tilde{\rho}_s \tilde{c}_s\left(-\frac{\partial \tilde{x}_m}{\partial \tilde{t}}\right)\right]\tilde{T}_m\right\},\quad [11]$$

where the unit normal $\hat{n}_m$ has $\tilde{x}_1$-, $\tilde{x}_2$- and $\tilde{x}_3$-components $-G_m^{-1}(\partial \tilde{x}_m/\partial \tilde{x}_1)$, $-G_m^{-1}(\partial \tilde{x}_m/\partial \tilde{x}_2)$ and G_m^{-1}, respectively, the geometric factor G_m being given by

$$G_m = \sqrt{1 + (\partial \tilde{x}_m/\partial \tilde{x}_1)^2 + (\partial \tilde{x}_m/\partial \tilde{x}_2)^2}.\qquad [12]$$

The parameter $\tilde{\gamma}_s$ is the heat of melting of the solid at temperature $\tilde{T} = 0$, where $\tilde{\gamma}_s$ is negative when melting is endothermic (alternatively, $\tilde{\gamma}_s$ may be defined as the heat of melting at the temperature $\tilde{T}_m$, in which case the term proportional to $\tilde{T}_m$ on the righthand side of [11] would be absent). Thus, there are discontinuities in gradients of temperature and other variables at $\tilde{x}_3 = \tilde{x}_m$, but the variables themselves remain continuous across the interface.

The model just described is meant to be a reasonable representation of certain classes of materials, such as the nitramine propellant HMX, that satisfy the main assumptions outlined above. Typical values associated with the physical properties of two widely studied nitramines,

HMX and RDX, were quoted in Mitani & Williams (1988) and in Li *et al.* (1990). Some of the approximations introduced above, such as the assumption of temperature equilibrium between phases, represent reasonable limiting cases, with order-of-magnitude estimates suggesting in particular that effects due to departures from the single-temperature limit are small in nitramine deflagration. Finally, although the present analysis is performed for the case of an unconfined deflagration, which is certainly of physical interest, the model itself allows for the analysis of confined deflagrations as well, as evidenced by the appearance of the pressure-derivative terms in [5] and [6].

3. NON-DIMENSIONALIZATION

The preceding formulation is given in terms of dimensional variables (identified by tildes). For the greatest convenience and generality, analyses are best performed using a suitable set of non-dimensional variables. For the present problem, an efficient selection is

$$x_i = \frac{\tilde{\rho}_s \tilde{c}_s \tilde{U}}{\tilde{\lambda}_s} \tilde{x}_i, \quad t = \frac{\tilde{\rho}_s \tilde{c}_s \tilde{U}^2}{\tilde{\lambda}_s} \tilde{t}, \quad T = \frac{\tilde{T}}{\tilde{T}_u}, \quad u_{L,G} = \frac{\tilde{u}_{L,G}}{\tilde{U}}, \quad \rho_G = \frac{\tilde{\rho}_G}{\tilde{\rho}_G^u}, \tag{13}$$

where the characteristic velocity $\tilde{U}$ is taken to be the speed of propagation $-d\tilde{x}_m/d\tilde{t}$ of a steady, planar deflagration, an explicit asymptotic expression for which has been derived previously (Margolis & Williams 1995a) and is restated below. The reference density $\tilde{\rho}_G^u$ in the last of [13] denotes the gas density at the unburned temperature $\tilde{T}_u$, and, from [7], is given by $\tilde{\rho}_G^u = \tilde{\rho}_G^\circ \tilde{W}_G/\tilde{R}^\circ \tilde{T}_u$.

The introduction of the non-dimensional variables defined above into the formulation presented in the preceding section results in a number of non-dimensional parameters. As in our previous studies (Margolis & Williams 1995a, b), these may be defined as

$$r = \frac{\tilde{\rho}_L}{\tilde{\rho}_s}, \quad \hat{r} = \frac{\tilde{\rho}_G^u}{\tilde{\rho}_s}, \quad l = \frac{\tilde{\lambda}_L}{\tilde{\lambda}_s}, \quad \hat{l} = \frac{\tilde{\lambda}_G}{\tilde{\lambda}_s}, \quad b = \frac{\tilde{c}_L}{\tilde{c}_s}, \quad \hat{b} = \frac{\tilde{c}_G}{\tilde{c}_s},$$

$$\gamma_s = \frac{\tilde{\gamma}_s}{\tilde{c}_s \tilde{T}_u}, \quad Q = \frac{\tilde{Q}}{\tilde{c}_s \tilde{T}_u}, \quad N = \frac{\tilde{E}}{\tilde{R}^\circ \tilde{T}_b}, \quad \Lambda = \frac{\tilde{\lambda}_s \tilde{A}}{\tilde{\rho}_s \tilde{c}_s \tilde{U}^2} e^{-N}, \tag{14}$$

where constant values for heat capacities and thermal conductivities have now been implicitly assumed. The last two parameters defined in [14] are reaction-rate parameters, N being a non-dimensional activation energy and Λ a non-dimensional burning-rate eigenvalue that enables the characteristic propagation speed $\tilde{U}$ to be determined from its definition and its value. We note that, in the analysis that follows, Q will be treated as a constant, even though this is strictly true only when $b = \hat{b}$, which is often a realistic approximation. These non-dimensional variables and parameters will be used from now on in this paper, and [1]–[12] are transformed accordingly.

4. THE OUTER PROBLEM

In the limit of large activation energy, the reaction zone collapses to a reaction front located at $x_3 = x_r(x_1, x_2, t) > x_m(x_1, x_2, t)$, and it is convenient to transform to the (non-orthogonal) moving co-ordinate

$$\zeta = x_3 - x_r(x_1, x_2, t) \tag{15}$$

whose origin is thus defined to be at $x_3 = x_r$. Introducing this transformation and the above non-dimensionalizations, the problem defined by [1]–[12] becomes

$$u_L = -\frac{\partial x_m}{\partial t} \left(\frac{1}{r} - 1 \right), \tag{16}$$

$$\frac{\partial \rho_G}{\partial t} + \frac{\partial}{\partial \zeta} \left[\rho_G \left(u_G - \frac{\partial x_r}{\partial t} \right) \right] = 0, \quad \zeta < -(x_r - x_m), \tag{17}$$

$$\frac{\partial}{\partial t}\left[\epsilon(\hat{r}\rho_G - r)\right] + \frac{\partial}{\partial\zeta}\left[r(1-\epsilon)\left(u_L - \frac{\partial x_r}{\partial t}\right) + \hat{r}\epsilon\rho_G\left(u_G - \frac{\partial x_r}{\partial t}\right)\right] = 0, \quad \zeta > -(x_r - x_m), \quad [18]$$

$$\frac{\partial\epsilon}{\partial t} - \frac{\partial}{\partial\zeta}\left[(1-\epsilon)\left(u_L - \frac{\partial x_r}{\partial r}\right)\right] = \Lambda(1-\epsilon)\exp\left[N\left(1 - \frac{T_b}{T}\right)\right], \quad \zeta > -(x_r - x_m), \quad [19]$$

$$\frac{\partial}{\partial t}\left\{[1-\epsilon_s) + \hat{r}\hat{b}\epsilon_s\rho_G]T\right\} + \frac{\partial}{\partial\zeta}\left\{\left[(1-\epsilon_s)\left(-\frac{\partial x_r}{\partial t}\right) + \hat{r}\hat{b}\epsilon_s\left(u_G - \frac{\partial x_r}{\partial t}\right)\rho_G\right]T\right\}$$

$$= \nabla_r \cdot \{[1 - \epsilon_s + \hat{l}\epsilon_s]\nabla_r T\}, \quad \zeta < -(x_r - x_m), \quad [20]$$

$$\frac{\partial}{\partial t}\left[r(1-\epsilon)(Q + bT) + \hat{r}\hat{b}\epsilon\rho_G T\right] + \frac{\partial}{\partial\zeta}\left[r(1-\epsilon)\left(u_L - \frac{\partial x_r}{\partial t}\right)(Q + bT) + \hat{r}\hat{b}\epsilon\left(u_G - \frac{\partial x_r}{\partial t}\right)\rho_G T\right]$$

$$= \nabla_r \cdot \{[l(1-\epsilon) + \hat{l}\epsilon]\nabla_r T\}, \quad \zeta > -(x_r - x_m), \quad [21]$$

$$\rho_G T = 1, \quad [22]$$

subject to

$$\epsilon = \epsilon_s \quad \text{for} \quad \zeta < -(x_r - x_m); \quad u_G \to 0, \quad T \to 1 \quad \text{as} \quad \zeta \to -\infty, \quad [23]$$

$$\epsilon \to 1, \quad T \to T_b \quad \text{as} \quad \zeta \to +\infty, \quad [24]$$

$$\epsilon|_{\zeta = -(x_r - x_m)} = \epsilon_s, \quad T|_{\zeta = -(x_r - x_m)} = T_m, \quad [25]$$

$$[l(1-\epsilon_s) + \tilde{l}\epsilon_s]\hat{n}_m \cdot \nabla_r T|_{\zeta = -(x_r - x_m)+} - (1-\epsilon_s) + \hat{l}\epsilon_s)\hat{n}_m \cdot \nabla_r T|_{\zeta = -(x_r - x_m)-}$$

$$= -G_m^{-1}\frac{\partial x_m}{\partial t}(1-\epsilon_s)(-\gamma_s + (b-1)T_m). \quad [26]$$

Here, ∇_r is the non-dimensional gradient operator expressed in terms of the moving co-ordinate system attached to the reacting surface, the x_1-, x_2- and x_3-components of which are given by

$$\nabla_r = \left(\frac{\partial}{\partial x_1} - \frac{\partial x_r}{\partial x_1}\frac{\partial}{\partial\zeta}, \frac{\partial}{\partial x_2} - \frac{\partial x_r}{\partial x_2}\frac{\partial}{\partial\zeta}, \frac{\partial}{\partial\zeta}\right). \quad [27]$$

The point of departure from our previous study (Margolis & Williams 1995b) resides in [22], since the earlier analysis was performed for the trivial equation of state $\rho_G = 1$, corresponding to constant gas density, while the present analysis allows for ideal gas-phase compressibility. The special case of steady, planar deflagration (Margolis & Williams 1995a) is recovered from this formulation by setting partial derivatives with respect to time and the transverse spatial co-ordinates (x_2, x_3) to zero. This basic solution is written down explicitly below, but for the present we note that the final burned temperature T_b that appears in the boundary condition [24] for the general non-steady, non-planar problem may be readily calculated from this special case as

$$T_b = \frac{(1-\epsilon_s)(Q + 1 + \gamma_s) + \hat{r}\hat{b}\epsilon_s}{\hat{b}[1 + \epsilon_s(\hat{r} - 1)]}. \quad [28]$$

This result is valid for both constant gas density and the compressible equation of state [22], as well as for the more general two-temperature case in which the rates of interphase heat transfer are finite (Margolis & Williams 1995a).

For additional simplicity in analyzing the effects of gas-phase compressibility on the stability of the deflagration, we shall assume that the gas-phase is quasi-steady with respect to the instantaneous reaction-front position $x_3 = x_r(x_1, x_2, t)$ (i.e. $\zeta = 0$ in the moving co-ordinate system). As a result, time derivatives of gas-phase variables are neglected in [17]–[21]. This assumption can be formally justified in the limit that $\dot{r}$ is small by introducing additional (short) characteristic temporal and spatial scales associated with the gaseous phase, which imply a larger characteristic velocity for the gaseous phase relative to condensed-phase velocities. With such a rescaling, gas-phase quantities are functions of their natural (short) space and time variables, and in addition, are functions of the longer condensed-phase space variables due to the forcing on that scale that arises from condensed-phase processes. In the quasi-steady approximation, it is implicitly assumed that only variations on the longer spatial and temporal scales associated with the condensed phase are of interest, leading to the absence of time derivatives of gas-phase quantities, which evolve only on the short gas-phase time scale. Thus, on the condensed spatial and temporal scales, the non-dimensional velocity $u_G - \partial x_r / \partial t$ becomes a relatively large quantity, of order $1/\dot{r}$. Restoring [17] to its original form through multiplication by $\dot{r}$, it is seen that the second term, being of order unity, dominates the first term, which is of order $\dot{r}$. Hence, all non-convective terms in [17]–[21] that are multiplied by $\dot{r}$ get dropped, and these terms are precisely the time derivatives of gas-phase quantities. That is, the gas phase responds to the local generation of additional gas in the reaction zone on a much faster time scale than that which governs the dynamics of the condensed phases. Although the assumption of gas-phase quasi-steadiness is well-established in studies of intrinsic combustion instability [cf. Denison & Baum (1961) and the recent reviews by De Luca (1992) and De Luca et al. (1995)], it is important to note that ignoring the dynamics that occur on the shorter gas-phase time scale does filter out any intrinsic dynamics associated with gas-phase processes. Indeed, such dynamics can be of the same order of magnitude as the dynamics associated with the condensed phase, examples being the diffusional/thermal and hydrodynamic instabilities that, just as in ordinary premixed flames, can occur in solid-propellant flames (cf. Margolis & Williams 1988, 1989). Nonetheless, assuming that intrinsic instabilities associated with the condensed and gaseous phases do not occur in the same parameter regimes, the quasi-steady approximation for the gas phase is useful for simplifying the analysis of the condensed-phase dynamics, while still allowing for an appropriate coupling with gas-phase quantities.

As has already been anticipated in our introduction of the moving coordinate ζ, we consider the limit of large activation energy $(N \gg 1)$, in which case all chemical activity and heat release associated with the reaction term in [19] are confined to a thin $O(N^{-1})$ reaction zone at $\zeta = 0$. In this way, the original distributed-reaction problem is reduced to a pair of reactionless problems in the outer regions $\zeta < 0$ and $\zeta > 0$, the solutions of which must be matched to the reaction-zone solution valid in the thin inner region $|\zeta| \ll 1$. The result is an asymptotic model for the outer variables, subject to nonlinear jump conditions across $\zeta = 0$ that depend on local conditions there, and an evolution equation for $x_r(x_1, x_2, t)$.

The outer solution for the gas-phase volume fraction and velocity is given by

$$\epsilon = \begin{cases} \epsilon_s, & \zeta < 0 \\ 1, & \zeta > 0, \end{cases} \tag{29}$$

$$u_G = \begin{cases} -(T-1)\partial x_r/\partial t, & \zeta < 0 \\ Tg(x_1, x_2, t) + \partial x_r/\partial t, & \zeta > 0, \end{cases} \tag{30}$$

where the first of these indicates that all variation in the volume-fraction variable ϵ is confined to the inner zone analyzed in the next section. Equation [30] follows from the neglect of gas-phase time derivatives owing to the quasi-steady assumption for that phase. Thus, u_G is given in terms of the local temperature and the instantaneous propagation speed of the reaction zone, with the "constant" of integration $g(x_1, x_2, t)$ to be determined. By use of these results and the equation

of state [22] in [20] and [21], and the neglect of all gas-phase time derivaties, the outer problem becomes

$$(1 - \epsilon_s)\frac{\partial T}{\partial t} + (1 - \epsilon_s + \hat{r}\hat{b}\epsilon_s)\left(-\frac{\partial x_r}{\partial t}\right)\frac{\partial T}{\partial t} = (1 - \epsilon_s + \hat{l}\epsilon_s)\nabla_r^2 T, \quad \zeta < -(x_r - x_m), \qquad [31]$$

$$rb(1 - \epsilon_s)\frac{\partial T}{\partial t} + [rb(1 - \epsilon_s) + \hat{r}\hat{b}\epsilon_s]\left(-\frac{\partial x_r}{\partial t}\right)\frac{\partial T}{\partial \zeta} - b(1 - r)(1 - \epsilon_s)\frac{\partial x_m}{\partial t}\frac{\partial T}{\partial \zeta}$$
$$= [l(1 - \epsilon_s) + \hat{l}\epsilon_s]\nabla_r^2 T, \quad -(x_r - x_m) < \zeta < 0, \qquad [32]$$

$$\hat{r}\hat{b}g\frac{\partial T}{\partial \zeta} = \hat{l}\nabla_r^2 T, \quad \zeta > 0, \qquad [33]$$

subject to the boundary conditions $T \to 1$ as $\zeta \to -\infty$ and $T \to T_b$ as $\zeta \to +\infty$, plus the continuity and jump conditions $T = T_m$ and [26] at $\zeta = -(x_r - x_m)$. From the expression [27] for ∇_r, the Laplacian operator ∇_r^2 in the (x_1, x_2, ζ) co-ordinate system is given by

$$\nabla_r^2 = \frac{\partial^2}{\partial x_1^2} + \frac{\partial^2}{\partial x_2^2} + G_r^2\frac{\partial^2}{\partial \zeta^2} - 2\frac{\partial x_r}{\partial x_1}\frac{\partial^2}{\partial x_1 \partial \zeta} - 2\frac{\partial x_r}{\partial x_2}\frac{\partial^2}{\partial x_2 \partial \zeta} - \left(\frac{\partial^2 x_r}{\partial x_1^2} + \frac{\partial^2 x_r}{\partial x_2^2}\right)\frac{\partial}{\partial \zeta}, \qquad [34]$$

where

$$G_r = \sqrt{1 + (\partial x_r/\partial x_1)^2 + (\partial x_r/\partial x_2)^2}. \qquad [35]$$

These conditions, however, are still not sufficient to completely determine the solution for the outer variables. To do so requires additional jump and continuity conditions across the thin reaction zone located at $\zeta = 0$, as well as an expression for the gas-velocity function $g(x_1, x_2, t)$ in the region $\zeta > 0$, which necessitates an analysis of the inner reaction-zone problem.

The derivation of two of the additional conditions needed to close the outer problem may be obtained directly from an integration of [21] across the thin reaction region; i.e. from $\zeta = 0^-$ to $\zeta = 0^+$. Using the results [29] and [30], and accounting for the fact that quantities such as ϵ, T, $\epsilon u_G T$, ϵT, $(1 - \epsilon)T$, $\epsilon \partial T/\partial \zeta$ and $(1 - \epsilon)\partial T/\partial \zeta$ behave, in the limit of large activation energy, as distributions there, the continuity and jump relations

$$T|_{\zeta = 0^-} = T|_{\zeta = 0^+} \qquad [36]$$

and

$$\left\{\hat{r}\hat{b}g + [(1 - \epsilon_s)rb + \epsilon_s\hat{r}\hat{b}]\frac{\partial x_r}{\partial t} + (1 - \epsilon_s)(1 - r)b\frac{\partial x_m}{\partial t}\right\}T|_{\zeta = 0} + (1 - \epsilon_s)Q\left[r\frac{\partial x_r}{\partial t} + (1 - r)\frac{\partial x_m}{\partial t}\right]$$
$$- (l - \hat{i})(1 - \epsilon_s)\left(\frac{\partial x_r}{\partial x_1}\frac{\partial T}{\partial x_1} + \frac{\partial x_r}{\partial x_2}\frac{\partial T}{\partial x_2}\right)\bigg|_{\zeta = 0} = G_r^2\left\{\hat{l}\frac{\partial T}{\partial \zeta}\bigg|_{\zeta = 0^+} - [l(1 - \epsilon_s) + \hat{l}\epsilon_s]\frac{\partial T}{\partial \zeta}\bigg|_{\zeta = 0^-}\right\} \qquad [37]$$

are obtained. The structure of the inner reaction zone, with suitable matching of solutions in that region to the outer solutions, must now be addressed to obtain an additional jump condition across $\zeta = 0$ and an expression for the function g introduced in [30]. We thus emply the method of matched asymptotic expansions and seek solutions to the outer problems in the form of the expansions $T \sim T^{(0)} + N^{-1}T^{(1)} + N^{-2}T^{(2)} + \cdots$, and similarly for the gas-velocity function g. Hence, to leading order, the outer equations obtained thus far are given by [26]–[37] with T and g replaced by $T^{(0)}$ and $g^{(0)}$, respectively.

5. THE REACTION-ZONE SOLUTIONS

Spatial variations in the reaction-zone solutions in the normal (ζ) direction occur on a short, of order N^{-1}, length scale relative to that of the outer solutions. Accordingly, it is appropriate to introduce the stretched normal co-ordinate η defined by

$$\eta = \beta\zeta = \beta(x_3 - x_r), \quad \beta = (1 - T_b^{-1})N, \qquad [38]$$

where β is the Zel'dovich number, and it is also convenient to introduce the normalized temperature variable $\Theta \equiv (T-1)/(T_b-1)$. Solutions to the inner problem are then sought in the form of the expansions

$$\epsilon \sim \epsilon_0 + \beta^{-1}\epsilon_1 + \beta^{-2}\epsilon_2 + \cdots,$$

$$u_G \sim u_0 + \beta^{-1}u_1 + \beta^{-2}u_2 + \cdots,$$

$$\Theta \sim 1 + \beta^{-1}\theta_1 + \beta^{-2}\theta_2 + \cdots,$$

$$\Lambda \sim \beta(\Lambda_0 + \beta^{-1}\Lambda_1 + \beta^{-2}\Lambda_2 + \cdots), \qquad [39]$$

where the latter represents the appropriate expansion of the burning-rate eigenvalue of the basic solution corresponding to steady, planar burning. Substituting these expansions and definitions into [18], [19] and [21] and equating coefficients of like powers of β, we obtain the leading-order inner problem in the following fashion. With [16] for u_L, [18] gives

$$\left(r - \frac{\hat{r}}{T_b}\right)\frac{\partial x_r}{\partial t}\frac{\partial \epsilon_0}{\partial \eta} + (1-r)\frac{\partial x_m}{\partial t}\frac{\partial \epsilon_0}{\partial \eta} + \frac{\hat{r}}{T_b}\frac{\partial}{\partial \eta}(\epsilon_0 u_0) = 0. \qquad [40]$$

Integrating this result and applying the matching conditions $\epsilon_0 \to \epsilon_s$ and $u_0 \to -(T_b-1)\,\partial x_r/\partial t$ as $\eta \to -\infty$, we obtain an expression for u_0 as

$$u_0 = \frac{T_b(\epsilon_0 - \epsilon_s)}{\hat{r}\epsilon_0}\left[(\hat{r}-r)\frac{\partial x_r}{\partial t} - (1-r)\frac{\partial x_m}{\partial t}\right] - (T_b-1)\frac{\partial x_r}{\partial t}. \qquad [41]$$

This result differs from that in Margolis & Williams (1995b) for constant gas-phase density, but the corresponding formula for that case can be obtained from [41] by setting $T_b = 1$. That is, the gas velocities with and without gas-phase thermal expansion differ by an amount proportional to the temperature rise $T_b - 1$. From the matching conditions $\epsilon_0 \to 1$ and $u_0 \to T_b g^{(0)} + \partial x_r/\partial t$ as $\eta \to +\infty$, an expression for the outer gas-velocity function $g^{(0)}(x_1, x_2, t)$ in the region $\zeta > 0$ is then found to be

$$g^{(0)}(x_1, x_2, t) = \frac{1-\epsilon_s}{\hat{r}}\left[(\hat{r}-r)\frac{\partial x_r}{\partial t} - (1-r)\frac{\partial x_m}{\partial t}\right] - \frac{\partial x_r}{\partial t}, \qquad [42]$$

which is needed in [33].

Utilizing [16] and [41] for the liquid and gas velocities, respectively, we find that the remaining part of the leading-order inner problem for ϵ_0 and θ_1 is now determined from [19] and [21] as

$$\left[r\frac{\partial x_r}{\partial t} + (1-r)\frac{\partial x_m}{\partial t}\right]\frac{\partial \epsilon_0}{\partial \eta} = -r\Lambda_0(1-\epsilon_0)e^{\theta_1}, \qquad [43]$$

$$\left[r\frac{\partial x_r}{\partial t} + (1-r)\frac{\partial x_m}{\partial t}\right][Q + (b-\hat{b})T_b]\frac{\partial \epsilon_0}{\partial \eta} = (T_b-1)G_r^2\frac{\partial}{\partial \eta}\left\{[l + (\hat{l}-l)\epsilon_0]\frac{\partial \theta_1}{\partial \eta}\right\}, \qquad [44]$$

subject to the matching conditions

$$\epsilon_0 \to 1, \quad \theta_1 \sim \Theta^{(1)}\big|_{\zeta = 0+} \quad \text{as} \quad \eta \to +\infty \qquad [45]$$

and

$$\epsilon_0 \to \epsilon_s, \quad \theta_1 \sim \Theta^{(1)}\big|_{\zeta = 0-} + \eta\frac{\partial \Theta^{(0)}}{\partial \zeta}\bigg|_{\zeta = 0-} \quad \text{as} \quad \eta \to -\infty, \qquad [46]$$

where, consistent with the definition of Θ, the $\Theta^{(i)}$ are defined as $\Theta^{(i)} = (T^{(i)} - 1)/(T_b - 1)$. We note that since spatial variations in the normal (ζ) direction are large relative to those in the transverse direction and those with respect to time, as reflected in the transformation [38], the reaction-zone problem [43]–[46] is always quasi-steady and quasi-planar, independent of the assumption of quasi-steadiness for the outer gas-phase equations introduced in the previous section. Thus, integrating [44] using [45], and then transforming to ϵ_0 as the independent co-ordinate according to [43], we obtain a first-order equation for θ_1 given by

$$r\Lambda_0 e^{\theta_1}\frac{\partial \theta_1}{\partial \epsilon_0} = H_{m,r}^2\frac{Q + (b-\hat{b})T_b}{T_b - 1} \cdot \frac{1}{l + (\hat{l}-l)\epsilon_0}. \qquad [47]$$

where

$$H_{m,r} = -G_r^{-1}\left[r\frac{\partial x_r}{\partial t} + (1-r)\frac{\partial x_m}{\partial t}\right].$$ [48]

Equation [47] may then be integrated with respect to ϵ_0 by using [46] to give

$$rA_0 e^{\theta_1} = H_{m,r}^2 \frac{Q+(b-\hat{b})T_b}{T_b-1} \cdot \begin{cases} (\hat{l}-l)^{-1}\{\ln[l+(\hat{l}-l)\epsilon_0] - \ln[l+(\hat{l}-l)\epsilon_s]\}, & \hat{l}\neq l \\ l^{-1}(\epsilon_0 - \epsilon_s), & \hat{l}=l. \end{cases}$$ [49]

For the special case of steady, planar burning, $\partial x_m/\partial t = \partial x_r/\partial t = -1$, and $\Theta^{(1)}|_{\zeta=0+} = 0$ in the matching condition [45]. Since [49] must hold for all solutions, these conditions determine the leading-order coefficient A_0 in the expansion [39] for the burning-rate eigenvalue as

$$A_0 = \frac{Q+(b-\hat{b})T_b}{r(T_b-1)} \cdot \begin{cases} (\hat{l}-l)^{-1}\{\ln\hat{l} - \ln[l+(\hat{l}-l)\epsilon_s]\}, & \hat{l}\neq l \\ l^{-1}(1-\epsilon_s), & \hat{l}=l, \end{cases}$$ [50]

in agreement with the result obtained from the steady-state analysis in Margolis & Williams (1995a). Here, T_b was given in [28], a result that in fact applies for the general non-steady, non-planar problem. An alternative expression for T_b in terms of γ_m, the non-dimensional endothermic heat of melting of the solid at temperature T_m, is

$$T_b = \frac{(1-\epsilon_s)[Q+1+(b-1)T_m - \gamma_m] + \hat{r}\hat{b}\epsilon_s}{\hat{b}[1+\epsilon_s(\hat{r}-1)]},$$ [51]

and can be derived in an analogous fashion from the steady-state version of [16]–[26] when the factor $-\gamma_s + (b-1)T_m$ is appropriately replaced by simply γ_m in the interface condition [26].

For the general non-steady, non-planar problem, [49], [50] and the matching condition [45] yield the local temperature-dependent propagation law

$$H_{m,r} = \exp(\tfrac{1}{2}\Theta^1|_{\zeta=0+}).$$ [52]

Equation [52] introduces the next-order outer variable Θ^1 into the analysis, but this additional complication, which is fundamental to this type of analysis (cf. Margolis & Williams 1989), can be circumvented in an approximate fashion by truncating the inner expansion [39] for Θ after the $O(\beta^{-1})$ term, so that the matching condition [45] implies that $\Theta^{(1)}|_{\zeta=0} = \beta(\Theta|_{\zeta=0} - 1)$. Reverting back to the original outer temperature variable T, we find that [52] may be expressed as

$$-r\frac{\partial x_r}{\partial t} - (1-r)\frac{\partial x_m}{\partial t} = \left[1 + \left(\frac{\partial x_r}{\partial x_1}\right)^2 + \left(\frac{\partial x_r}{\partial x_2}\right)^2\right]^{1/2}\exp\left(-\frac{\beta}{2}\cdot\frac{T_b-T|_{\zeta=0}}{T_b-1}\right),$$ [53]

where we have used the definition [48] for $H_{m,r}$. Substitution of [53] and the expression [42] for g into [37] then leads to the result

$$\hat{l}\frac{\partial T}{\partial\zeta}\bigg|_{\zeta=0+} - [l+(\hat{l}-l)\epsilon_s]\frac{\partial T}{\partial\zeta}\bigg|_{\zeta=0-} + (1-\epsilon_s)(l-\hat{l})G_r^{-2}\left(\frac{\partial x_r}{\partial x_1}\frac{\partial T}{\partial x_1} + \frac{\partial x_r}{\partial x_2}\frac{\partial T}{\partial x_2}\right)\bigg|_{\zeta=0}$$

$$= -(1-\epsilon_s)[Q+(b-\hat{b})T|_{\zeta=0}]G_r^{-1}\exp\left(-\frac{\beta}{2}\cdot\frac{T_b-T|_{\zeta=0}}{T_b-1}\right),$$ [54]

which, if we retain [53], replaces [37] as the required jump condition across the thin reaction zone. When the outer solution is approximated (truncated) by setting $T\approx T^{(0)}$ and $g\approx g^{(0)}$, the derived conditions [36] and [37], the propagation law [53], and the expression [42] for the outer gas-velocity function g close the outer problem [23]–[26], [29]–[33]. We observe that, despite differences in the expression for the gas velocity, [53] and [54] are identical to those obtained from the corresponding analysis (Margolis & Williams 1995b) for the case of constant gas density.

6. SUMMARY OF THE ASYMPTOTIC MODEL AND ITS BASIC SOLUTION

The model derived in the previous two sections constitutes an asymptotic formulation, valid for large activation energies, of deflagration in porous energetic materials for the case of a thermally

expansive, quasi-steady gas phase. In this regime, the reaction zone becomes thin relative to the convective–diffusive structure of the deflagration wave, in such a way that both the jump condition across the reaction sheet and the propagation law that governs its motion display a sensitivity to local temperature perturbations. This sensitivity is of a finite, but exponential, form that is induced by the original Arrhenius nature of the reaction rate in the asymptotic limit described above. It is helpful to collect the above results for future reference. Hence, the asymptotic mode, expressed in non-orthogonal co-ordinates (x_1, x_2, ζ) attached to the reaction surface ($\zeta = 0$), is given by

$$(1 - \epsilon_s)\begin{Bmatrix} 1 \\ rb \\ 0 \end{Bmatrix}\frac{\partial T}{\partial t} - \begin{Bmatrix} 1 + \epsilon_s(\hat{r}\hat{b} - 1) \\ rb + \epsilon_s(\hat{r}\hat{b} - rb) \\ \hat{r}\hat{b} \end{Bmatrix}\frac{\partial x_r}{\partial t}\frac{\partial T}{\partial \zeta} - (1 - \epsilon_s)\left[(1 - r)\begin{Bmatrix} 0 \\ b \\ \hat{b} \end{Bmatrix}\frac{\partial x_m}{\partial t} + (r - \hat{r})\begin{Bmatrix} 0 \\ 0 \\ \hat{b} \end{Bmatrix}\frac{\partial x_r}{\partial t}\right]\frac{\partial T}{\partial \zeta}$$

$$= \begin{Bmatrix} 1 + \epsilon_s(\hat{l} - 1) \\ l + \epsilon_s(\hat{l} - l) \\ \hat{l} \end{Bmatrix}\nabla_r^2 T, \quad \begin{matrix} \zeta < -(x_r - x_m) \\ -(x_r - x_m) < \zeta < 0 , \\ \zeta > 0 \end{matrix} \quad [55]$$

$$-r\frac{\partial x_r}{\partial t} - (1 - r)\frac{\partial x_m}{\partial t} = G_r \exp\left(-\frac{\beta}{2} \cdot \frac{T_b - T|_{\zeta = 0}}{T_b - 1}\right), \quad [56]$$

subject to

$$T \to 1 \text{ as } \zeta \to -\infty, \quad T \to T_b \text{ as } \zeta \to +\infty, \quad T = T_m \text{ at } \zeta = -(x_r - x_m), \quad [57]$$

$$\left(-\frac{\partial x_m}{\partial x_1}, -\frac{\partial x_m}{\partial x_2}, 1\right) \cdot \{[l + \epsilon_s(\hat{l} - l)]\nabla_r T|_{\zeta = -(x_r - x_m)^+} - [1 + \epsilon_s(\hat{l} - 1)]\nabla_r T|_{\zeta = -(x_r - x_m)^-}\}$$

$$= -\frac{\partial x_m}{\partial t}(1 - \epsilon_s)[-\gamma_s + (b - 1)T_m], \quad [58]$$

$$T|_{\zeta = 0^-} = T|_{\zeta = 0^+}, \quad [59]$$

$$\hat{l}\frac{\partial T}{\partial \zeta}\Big|_{\zeta = 0^+} - [l + (\hat{l} - l)\epsilon_s]\frac{\partial T}{\partial \zeta}\Big|_{\zeta = 0^-} + (1 - \epsilon_s)(l - \hat{l})G_r^{-2}\left(\frac{\partial x_r}{\partial x_1}\frac{\partial T}{\partial x_1} + \frac{\partial x_r}{\partial x_2}\frac{\partial T}{\partial x_2}\right)\Big|_{\zeta = 0}$$

$$= -(1 - \epsilon_s)[Q + (b - \hat{b})T|_{\zeta = 0}]G_r^{-1}\exp\left(-\frac{\beta}{2} \cdot \frac{T_b - T|_{\zeta = 0}}{T_b - 1}\right), \quad [60]$$

where the dot in [58] represents the scalar product of the vector on the left with the operator ∇_r given in [27], and where expressions for $\nabla_r^2 = \nabla_r \cdot \nabla_r$ and G_r were given in [34] and [35], respectively. Equations [55]–[60], which constitute a closed boundary-value problem for x_r, x_m and T, may be solved subject to arbitrary initial conditions. Here, however, we shall only be concerned with the long-time basic solution corresponding to a steady, planar deflagration, as described by the formulation derived in the previous section, and its stability. We note that other variables of interest, such as the gas velocity, are given in terms of x_r, x_m and T according to the formulae derived in the previous section.

A basic solution of the model [55]–[60], corresponding to a steadily propagating planar deflagration and denoted by a zero superscript, is given by

$$x_m^0 = -t, \quad x_r^0 = x_m^0 + \frac{l(1 - \epsilon_s) + \hat{l}\epsilon_s}{b(1 - \epsilon_s) + \hat{r}\hat{b}\epsilon_s}\ln\left(\frac{T_b - B}{T_m - B}\right), \quad [61]$$

$$T^0(\zeta) = \begin{cases} 1 + (T_m - 1)\exp\left[\dfrac{1 + \epsilon_s(\hat{r}\hat{b} - 1)}{1 + \epsilon_s(\hat{l} - 1)}(\zeta + x_r^0 - x_m^0)\right], & \zeta < -(x_r^0 - x_m^0) \\[2em] B + (T_m - B)\exp\left[\dfrac{b(1 - \epsilon_s) + \hat{r}\hat{b}\epsilon_s}{l(1 - \epsilon_s) + \hat{l}\epsilon_s}(\zeta + x_r^0 - x_m^0)\right], & -(x_r^0 - x_m^0) < \zeta < 0 \\[2em] T_b = \dfrac{(1 - \epsilon_s)(Q + 1 + \gamma_s) + \hat{r}\hat{b}\epsilon_s}{\hat{b}[1 + \epsilon_s(\hat{r} - 1)]}, & \zeta > 0, \end{cases} \quad [62]$$

where

$$B \equiv \frac{(1 - \epsilon_s)(1 + \gamma_s) + \hat{r}\hat{b}\epsilon_s}{b(1 - \epsilon_s) + \hat{r}\hat{b}\epsilon_s}.$$

[63]

In addition, from [30] and [42], the steady, planar gas-phase velocity u_G^0 is given by

$$u_G^0 = \begin{cases} T - 1, & \zeta < 0 \\ \hat{r}^{-1}[(1 - \hat{r})(1 - \epsilon_s) + (T_b - 1)(1 - \epsilon_s + \epsilon_s \hat{r})], & \zeta > 0. \end{cases}$$

[64]

Finally, the propagation speed of this solution is determined from the last of [14] and the derived expression [50] for the burning-rate eigenvalue. The various features of this solution as a function of the parameters in the problem were described in considerable detail in Margolis & Williams (1995a). Here, we are particularly interested in the effects of the porosity ϵ_s, in the realistic limit of small gas-to-solid density ratio $\hat{r}$, on the stability of steady, planar deflagration. As shown in the next section, the value of the burned temperature plays a critical role in determining the corresponding neutral stability boundary, in part because the propagation velocity is exponentially sensitive to T_b in this regime of large activation energy (see the last of [14]). From [28], T_b has the behavior

$$T_b = \frac{1}{\hat{b}}\left[Q + 1 + \gamma_s - \hat{r}\frac{\epsilon_s}{1 - \epsilon_s}(Q + 1 + \gamma_s - \hat{b}) + O(\hat{r}^2) \right],$$

[65]

for $\hat{r} \ll 1$. Since the non-dimensional heat release Q is typically significantly larger than unity, whereas the specific heat capacity ratio $\hat{b}$ is generally not significantly larger than unity, the final burned temperature, and hence the steady mass burning rate, decrease with increasing porosity and increasing gas density (Margolis & Williams 1995a).

7. LINEAR STABILITY ANALYSIS

Using the derived asymptotic model, the linear stability analysis of the basic solution [61]–[63] follows a standard approach and parallels our earlier (Margolis & Williams 1995a) stability analysis. Briefly, perturbation variables $\phi_m(x_1, x_2, t)$, $\phi_r(x_1, x_2, t)$ and $\tau(x_1, x_2, \zeta, t)$ are defined according to

$$x_m = x_m^0 + \phi_m, \quad x_r = x_r^0 + \phi_r, \quad T = T^0(\zeta) + \tau + \phi_r \frac{dT^0}{d\zeta}.$$

[66]

These definitions are substituted into the asymptotic model defined by [55]–[60], and the equations are linearized with respect to the perturbation variables to obtain a linear problem for ϕ_m, ϕ_r and τ given by

$$(1 - \epsilon_s)\frac{\partial \tau}{\partial t} + [1 + \epsilon_s(\hat{r}\hat{b} - 1)]\frac{\partial \tau}{\partial \zeta} = [1 + \epsilon_s(\hat{l} - 1)]\left(\frac{\partial^2 \tau}{\partial x_1^2} + \frac{\partial^2 \tau}{\partial x_2^2} + \frac{\partial^2 \tau}{\partial \zeta^2}\right), \quad \zeta < -(x_r^0 - x_m^0),$$

[67]

$$rb(1 - \epsilon_s)\frac{\partial \tau}{\partial t} + [b + \epsilon_s(\hat{r}\hat{b} - b)]\frac{\partial \tau}{\partial \zeta} - b(1 - r)(1 - \epsilon_s)\frac{\partial \phi_m}{\partial t}\frac{dT^0}{d\zeta}$$

$$= [l + \epsilon_s(\hat{l} - l)]\left(\frac{\partial^2 \tau}{\partial x_1^2} + \frac{\partial^2 \tau}{\partial x_2^2} + \frac{\partial^2 \tau}{\partial \zeta^2}\right), \quad -(x_r^0 - x_m^0) < \zeta < 0,$$

[68]

$$\hat{b}[1 + \epsilon_s(\hat{r} - 1)]\frac{\partial \tau}{\partial \zeta} = \hat{l}\left(\frac{\partial^2 \tau}{\partial x_1^2} + \frac{\partial^2 \tau}{\partial x_2^2} + \frac{\partial^2 \tau}{\partial \zeta^2}\right), \quad \zeta > 0,$$

[69]

$$-r\frac{\partial \phi_r}{\partial t} - (1 - r)\frac{\partial \phi_m}{\partial t} = \frac{\beta}{2(T_b - 1)}\tau|_{\zeta = 0+},$$

[70]

subject to

$$\tau \to 0 \quad \text{as} \quad \zeta \to \pm \infty,$$

[71]

$$\left(\tau + \phi_m \frac{dT^0}{d\zeta}\right)\Bigg|_{\zeta = -(x_r^0 - x_m^0)^-} = \left(\tau + \phi_m \frac{dT^0}{d\zeta}\right)\Bigg|_{\zeta = -(x_r^0 - x_m^0)^+} = 0, \qquad [72]$$

$$[l + \epsilon_s(\hat{l} - l)]\left(\frac{\partial \tau}{\partial \zeta} + \phi_m \frac{d^2 T^0}{d\zeta^2}\right)\Bigg|_{\zeta = -(x_r^0 - x_m^0)^+} - [1 + \epsilon_s(\hat{l} - 1)]\left(\frac{\partial \tau}{\partial \zeta} + \phi_m \frac{d^2 T^0}{d\zeta^2}\right)\Bigg|_{\zeta = -(x_r^0 - x_m^0)^-}$$

$$= -\frac{\partial \phi_m}{\partial t}(1 - \epsilon_s)[-\gamma_s + (b - 1)T_m], \quad [73]$$

$$\tau|_{\zeta = 0^-} = \left(\tau + \phi_r \frac{dT^0}{d\zeta}\right)\Bigg|_{\zeta = 0^-}, \qquad [74]$$

$$\hat{l}\frac{\partial \tau}{\partial \zeta}\Bigg|_{\zeta = 0^+} - [l + \epsilon_s(\hat{l} - l)]\left(\frac{\partial \tau}{\partial \zeta} + \phi_r \frac{d^2 T^0}{d\zeta^2}\right)\Bigg|_{\zeta = 0^-}$$

$$= -\frac{1}{2}(1 - \epsilon_s)\left[\frac{\beta Q}{T_b - 1} + (b - \hat{b})\left(2 + \frac{\beta T_b}{T_b - 1}\right)\right]\tau|_{\zeta = 0^+}, \quad [75]$$

where we have used the fact that $dT^0/d\zeta = 0$ for $\zeta > 0$.

From [66], steady, planar burning clearly corresponds to the trivial solution $\phi_m = \phi_r = \tau = 0$, whereas non-trivial solutions to the linear stability problem are sought in the form

$$\begin{Bmatrix} \phi_m \\ \phi_r \\ \tau \end{Bmatrix} = e^{i(\omega t \pm k_1 x_1 \pm k_2 x_2)}\begin{Bmatrix} c_m \\ 1 \\ \sigma(\zeta) \end{Bmatrix}, \qquad [76]$$

which has been normalized by setting the coefficient of ϕ_r equal to unity. Equations [67]–[69] and [71] then determine the function $\sigma(\zeta)$ as

$$\sigma(\zeta) = \begin{cases} c_1 e^{p\zeta} & \zeta < -(x_r^0 - x_m^0) \\ c_2 e^{q_- \zeta} + c_3 e^{q_+ \zeta} + i\omega(i\omega \hat{b}_3 + k^2)^{-1}c_m b_2 b_4(T_m - B)e^{b_2 \zeta}, & -(x_r^0 - x_m^0) < \zeta < 0 \\ c_4 e^{\hat{s}\zeta}, & \zeta > 0, \end{cases}$$

$$[77]$$

where the c_i are constants of integration, and the other quantities that appear in [77] are given by

$$b_1 = \frac{1 + \epsilon_s(\hat{r}\hat{b} - 1)}{1 + \epsilon_s(\hat{l} - 1)}, \quad \hat{b}_1 = \frac{1 - \epsilon_s}{1 + \epsilon_s(\hat{l} - 1)}, \quad b_2 = \frac{b + \epsilon_s(\hat{r}\hat{b} - b)}{l + \epsilon_s(\hat{l} - l)},$$

$$\hat{b}_3 = \frac{rb(1 - \epsilon_s)}{l + \epsilon_s(\hat{l} - l)}, \quad b_4 = \frac{b(r - 1)(1 - \epsilon_s)}{l + \epsilon_s(\hat{l} - l)}, \quad b_5 = \frac{\hat{b}}{\hat{l}}[1 + \epsilon_s(\hat{r} - 1)], \qquad [78]$$

and

$$p = \frac{1}{2}\left[b_1 + \sqrt{b_1^2 + 4(i\omega \hat{b}_1 + k^2)}\right], \quad q_\pm = \frac{1}{2}\left[b_2 \pm \sqrt{b_2^2 + 4(i\omega \hat{b}_3 + k^2)}\right],$$

$$\hat{s} = \frac{1}{2}\left[b_5 - \sqrt{b_5^2 + 4k^2}\right]. \qquad [79]$$

The remaining conditions embodied in [70] and [72]–[75] serve to determine the c_i and the dispersion relation $\omega(k)$, where $k = \sqrt{k_1^2 + k_2^2}$.

8. ANALYSIS OF THE DISPERSION RELATION

The linear stability analysis is completed for a representative case in which $r = b = l = 1$, corresponding to the neglect of differences between the physical properties of the solid and liquid

phases of the material. While this restriction is introduced in order to reduce algebraic complexity, it clearly can be relaxed if there is interest in other values of these parameters. As a result, $b_1 = b_2$, $\acute{b}_1 = \acute{b}_3$ (which implies that $q_+ = p$) and $b_4 = 0$. Then, from [70] and [72]–[74], the coefficients in [77] are determined as

$$c_1 = -c_m b_1 (T_m - 1) e^{q_+ (x_r^0 - x_m^0)}, \quad c_2 = (B - 1) c_m b_1 \left(\frac{q_- + i\omega}{q_- - q_+} \right) e^{q_- (x_r^0 - x_m^0)},$$

$$c_3 = -c_m b_1 \left[T_m - 1 + (B - 1) \frac{q_+ + i\omega}{q_- - q_+} \right] e^{q_+ (x_r^0 - x_m^0)}, \quad c_4 = -2i\omega \frac{T_b - 1}{\beta}, \qquad [80]$$

where $x_r^0 - x_m^0$ was given by the second of [61] and

$$c_m = \frac{[(T_b - 1)(b_1 + 2i\omega/\beta) - (B - 1)b_1] e^{-q_+ (x_r^0 - x_m^0)}}{b_1(T_m - 1) - (B - 1)b_1(q_- - q_+)^{-1} [(q_- + i\omega) e^{(q_- - q_+)(x_r^0 - x_m^0)} - (q_+ + i\omega)]}. \qquad [81]$$

We remark that, in light of the above simplification, all effects due to melting of the solid are embodied in the parameter γ_s. In the limit that the heat of melting becomes negligible ($\gamma_s \to 0$), we have $B \to 1$ and hence $c_2 \to 0$. In that case, the functional form of the temperature function $\sigma(\zeta)$ is the same on either side of $\zeta = -(x_r^0 - x_m^0)$, and the melting surface becomes effectively "invisible".

An equation for the dispersion relation $\omega(k)$ is now obtained by substituting the results given thus far into [75]. The result is, in terms of the coefficients defined above,

$$\acute{l}s c_4 - (1 - \epsilon_s + \acute{l}\epsilon_s)[q_- c_2 + q_+ c_3 + b_1^2 (T_b - B)] = -(1 - \epsilon_s) \left[\beta \frac{Q + (1 - \acute{b}) T_b}{2(T_b - 1)} + 1 - \acute{b} \right] c_4, \qquad [82]$$

where s and $q_\pm$ depend on $i\omega$ and k according to their definitions given above. This is a fairly complicated dispersion relation, but typically, the gas density is small compared with that of the condensed phases, the thermal conductivity of the gas is correspondingly small, and the heat of melting is small compared with the thermal enthalpy. For these reasons, the gas-to-solid/liquid density ratio $\acute{r}$ is treated as a small parameter, and the scalings

$$\acute{l} = \acute{l}^* \acute{r}, \quad \gamma_s = \gamma_s^* \acute{r}. \qquad [83]$$

are introduced for the corresponding conductivity ratio $\acute{l}$ and the non-dimensional heat of melting γ_s, where the scaled values $\acute{l}^*$ and γ_s^* are considered to be of order unity. The dispersion relation $\omega(k)$ is then expanded as

$$\omega \sim \omega_0 + \omega_1 \acute{r} + \omega_2 \acute{r}^2 + \cdots. \qquad [84]$$

Associated expansions of all quantities in [82] that depend on these small parameters are then performed, keeping the overall heat release Q_0 with respect to the solid,

$$Q_0 = Q + \gamma_s, \qquad [85]$$

a fixed parameter. Under this constraint, there is an expansion of the burned temperature T_b according to [28] as

$$T_b \sim T_b^0 + \acute{r} T_b^1 + \cdots, \quad T_b^0 = \frac{Q_0 + 1}{\acute{b}}, \quad T_b^1 = -\frac{\epsilon_s}{1 - \epsilon_s}(T_b^0 - 1). \qquad [86]$$

In addition, the expansions

$$B - 1 \sim \gamma_s^* \acute{r}, \quad \acute{l}s \sim O(\acute{r}^2), \quad b_1 \sim 1 + \frac{\epsilon_s}{1 - \epsilon_s}(\acute{b} - \acute{l}^*) \acute{r} + \cdots, \quad \acute{b}_1 \sim 1 - \frac{\epsilon_s}{1 - \epsilon_s} \acute{l}^* \acute{r} + \cdots, \qquad [87]$$

and

$$q_\pm \sim q_\pm^0 + q_\pm^1 \acute{r} + \cdots, \quad q_\pm^0 = \frac{1}{2} \left[1 \pm \sqrt{1 + 4(i\omega_0 + k^2)} \right],$$

$$q_\pm^1 = \frac{1}{2} \cdot \frac{\epsilon_s}{1 - \epsilon_s} \left[\acute{b} - 2\acute{l}^* q_\pm^0 \pm \frac{\acute{b} + \acute{l}^* (2i\omega_0 + 4k^2)}{2q_+^0 - 1} \right] \pm \frac{i\omega_1}{2q_+^0 - 1} \qquad [88]$$
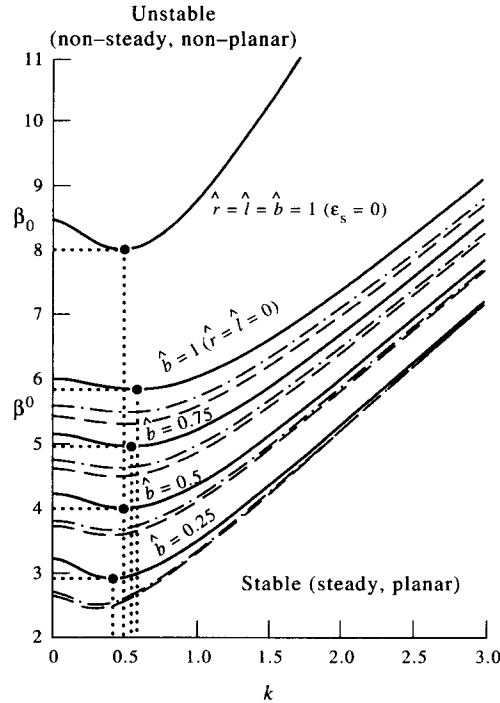
Figure 2. Leading-order neutral stability boundaries $\beta_0(k)$ (solid curves) as a function of wavenumber for several values of the gas-to-liquid/solid heat-capacity ratio $\hat{b}$. Also shown is the corresponding neutral stability boundary (top curve) for the strictly solid combustion–synthesis (SHS) problem, and the modified boundaries $\beta^0(k)$ (chain–dot and chain–dash curves for constant and non-constant gas density, respectively) that are obtained when the next-order correction with respect to $\hat{r}$ is included. The latter boundaries are calculated for reasonable values of the remaining parameters ($\epsilon_s = 0.3$, $\gamma_s = 0$, $\hat{r} = 0.1$, $\hat{l}^* = 1.0$, $T_b^0 = 6.0$).

apply. Substitution of these expansions into [82] determines the equation for the leading-order dispersion relation $\omega_0(k)$ to be $(2i\omega_0 + \beta)(1 - q_+^0) + i\omega(\beta - 2\hat{b})$ which, after some manipulation, can be expressed as

$$4(i\omega_0)^3 + (i\omega_0)^2[4k^2 + 4\hat{b}(1 - \hat{b}) + 2(1 + 2\hat{b})\beta - \beta^2)] + 2i\omega_0\beta(\hat{b} + 2k^2) + \beta^2k^2 = 0. \qquad [89]$$

This dispersion relation is identical to the result obtained previously (Margolis & Williams 1995b) when a constant density for the gas phase was assumed. It is therefore concluded that, in the first approximation for small values of $\hat{r}$, the gas-phase thermal expansion has no effect on the stability behavior, a result that might be anticipated based on the small contribution of the mass fraction of gas in this limit.

The neutral stability boundary, corresponding to neither growth nor decay of the infinitesimal perturbations of the form given by [76], can be displayed in a plane of the Zel'dovich number β, defined by the second of [38], and the non-dimensional wavenumber k. This boundary is obtained by setting the real part of the complex growth rate $i\omega$ to zero. By setting the real and imaginary parts of [89] separately to zero, the neutral stability boundary at leading order, $\beta_0(k)$, can be obtained as the positive root of the quadratic

$$(\hat{b} + 2k^2)\beta_0^2 + 2[k^2 - (1 + 2\hat{b})(\hat{b} + 2k^2)]\beta_0 - 4(\hat{b} + 2k^2)[\hat{b}(1 - \hat{b}) + k^2] = 0, \qquad [90]$$

and the corresponding leading-order frequency $\omega_0(k)$ of the neutral disturbance is

$$\omega_0^2 = \tfrac{1}{2}\beta_0(\hat{b} + 2k^2). \qquad [91]$$

Since $\omega_0 \neq 0$, the stability boundary is of the pulsating type, like that obtained by Denison & Baum (1961) and others (cf. Margolis & Armstrong 1986; Margolis & Williams 1988) for solid-propellant combustion in the absence of two-phase flow (such intrinsic pulsating instabilities are also observable experimentally; cf. Zanotti *et al.* 1992). This leading-order stability boundary was obtained and discussed previously (Margolis & Williams 1995b), and, for completeness, has been

included in figure 2 (solid curves), which also exhibits the next-order approximation for a modified Zel'dovich number $\beta^0(k)$ (chain–dash and chain–dot curves) as discussed below. Several curves, corresponding to different values of $\hat{b}$, are shown, indicating that decreasing values of $\hat{b}$ are destabilizing, which suggests that diminished thermal influences of the gas phase (which convects heat away from the reaction zone in the direction of the burned region) is less able to damp the known thermal/diffusive instability of the condensed phase (cf. Margolis 1991). Indeed, we also show for reference the neutral stability boundary corresponding to strictly condensed-phase combustion (combustion synthesis), which can be recovered from the present analysis by setting $\hat{r} = \hat{l} = \hat{b} = 1$ and $\epsilon_s = 0$ in [82]. This stability boundary, which is determined (in the absence of melting) from the dispersion relation

$$4(i\omega)^3 + (i\omega)^2[1 + 4k^2 + 2\beta - \tfrac{1}{4}\beta^2] + \tfrac{1}{2}(i\omega)(1 + 4k^2) + \tfrac{1}{4}\beta^2 k^2 = 0, \qquad [92]$$

is qualitatively similar to the stability boundaries obtained from [89], reflecting the fact that this particular type of instability phenomenon arises from combustion of the condensed phase, with the presence of the gas having a secondary, perturbative effect as discussed below. The fact that the minimum value of $\beta_0(k)$, given by $\beta_0 = 1 + 2\hat{b} + \sqrt{8\hat{b}}$, occurs at a non-zero value of $k = (\hat{b}/8)^{1/4} > 0$ (as compared with $\beta_0 = 1 + 2\hat{b} + \sqrt{1 + 8\hat{b}}$ at $k = 0$) suggests that non-planar, cellular patterns will be observed at the transition to non-steady burning as the stability boundary is crossed. Since the leading-order results for the neutral stability boundary are independent of the porosity ϵ_s, they are also the same as those obtained previously for the non-porous case (Margolis & Williams 1990) as well as for a different model in which two-phase flow effects were suppressed in favor of an intrusive gas flame adjacent to a pyrolyzing solid surface (Margolis & Armstrong 1986). Consequently, these same or very similar results are likely to occur in a variety of different energetic systems.

Since the leading-order results regarding the neutral stability boundary are independent of ϵ_s, to investigate the effects of non-zero porosity it is necessary to proceed to the next order in the ratio of gas density and conductivity to those of the condensed phases. With the neutral stability boundary thus represented as

$$\beta \sim \beta_0 + \beta_1 \hat{r} + \cdots, \qquad [93]$$

an expression for $\omega_1(k)$, introduced in [84], can be obtained from the dispersion relation at $O(\hat{r})$ given by

$$i\omega_1\left[\beta_0 + 2(1 - \hat{b} - q^0_+) - \frac{2i\omega_0 + \beta_0}{2q^0_+ - 1}\right] + \frac{2i\omega_0}{\beta_0}[q^0_+ - 1 + \hat{b})\beta_1 = \frac{\epsilon_s}{1 - \epsilon_s}\left\{\beta_0(1 - q^0_+)\hat{l}^* \right.$$

$$+ [\tfrac{1}{2}\beta_0(2q^0_+ - 3) - i\omega_0(\beta_0 - 1)]\hat{b} + \tfrac{1}{2} \cdot \frac{2i\omega_0 + \beta_0}{2q^0_+ - 1}[\hat{b} + (2i\omega_0 + 4k^2)\hat{l}^*]\right\}$$

$$- \gamma_s^*\left\{(T_b^0 - 1)^{-1}\left[\beta_0(i\omega_0 - q^0_-) - \frac{q^0_+}{\hat{b}}(2i\omega_0 + \beta_0)\right]\right.$$

$$+ (T_m - 1)^{-1}(i\omega_0 + q^0_-)(2i\omega_0 + \beta_0)e^{(q^0_- - q^0_+)\ln[T_b^0 - 1)/(T_m - 1)]}\right\}, \qquad [94]$$

where β_0 and ω_0 were given by [90] and [91], respectively. We observe that [94] differs from the corresponding result in our earlier study (Margolis & Williams 1995b) that assumed a constant gas density, and thus modifications in the neutral stability boundary due to thermal expansion of the gas appear at this order in the analysis. Setting $\mathrm{Re}(i\omega_1)$ to zero and equating real and imaginary parts of [94] separately to zero then gives a coupled system of linear equations for β_1 and ω_1 as

$$a_{1,1}\omega_1 + a_{1,2}\beta_1 = c_{1,1} + c_{1,2}\hat{l}^* + c_{1,3}\gamma_s^*$$

$$a_{2,1}\omega_1 + a_{2,2}\beta_1 = c_{2,1} + c_{2,2}\hat{l}^* + c_{2,3}\gamma_s^*, \qquad [95]$$

where

$$a_{1,1} = q_i + \frac{2\omega_0 q_r - \beta_0 q_i}{q_r^2 + q_i^2}, \quad a_{1,2} = -\frac{\omega_0 q_i}{\beta_0},$$ [96]

$$a_{2,1} = \beta_0 + 1 - 2\acute{b} - q_r - \frac{2\omega_0 q_i + \beta_0 q_r}{q_r^2 + q_i^2}, \quad a_{2,2} = \frac{\omega_0}{\beta_0}(q_r - 1 + 2\acute{b}),$$ [97]

$$c_{1,1} = -\frac{\epsilon_s}{1 - \epsilon_s} \cdot \frac{\acute{b}}{2}\left[(2 - q_r)\beta_0 - \frac{\beta_0 q_r + 2\omega_0 q_i}{q_r^2 + q_i^2}\right],$$ [98]

$$c_{1,2} = -\frac{\epsilon_s}{1 - \epsilon_s} \cdot \frac{1}{2}\left[(q_r - 1)\beta_0 - \frac{4(\beta_0 k^2 - \omega_0^2)q_r + 2\omega_0(\beta_0 + 4k^2)q_i}{q_r^2 + q_i^2}\right],$$ [99]

$$c_{1,3} = -\frac{1}{2\acute{b}(T_b^0 - 1)}\{2\omega_0 q_i + \beta_0[(\acute{b} - 1)q_r - \acute{b} - 1]\}$$

$$- \frac{1}{2(T_m - 1)}e^{-q_r \ln \gamma}\{[(1 - q_r)\beta_0 - 2\omega_0(2\omega_0 - q_i)]\cos(q_i \ln \gamma)$$

$$+ [(2\omega_0 - q_i)\beta_0 + 2\omega_0(1 - q_r)]\sin(q_i \ln \gamma)\},$$ [100]

$$c_{2,1} = -\frac{\epsilon_s}{1 - \epsilon_s} \cdot \frac{\acute{b}}{2}\left[2\omega_0(\beta_0 - 1) - \beta_0 q_i - \frac{2\omega_0 q_r - \beta_0 q_i}{q_r^2 + q_i^2}\right],$$ [101]

$$c_{2,2} = -\frac{\epsilon_s}{1 - \epsilon_s} \cdot \frac{1}{2}\left[(2 + q_i)\beta_0 - \frac{4(\omega_0 k^2 - \beta_0 k^2)q_i + 2\omega_0(\beta_0 + 4k^2)q_r}{q_r^2 + q_i^2}\right],$$ [102]

$$c_{2,3} = -\frac{1}{2\acute{b}(T_b^0 - 1)}\{-2\omega_0(1 + q_r) + \beta_0[(\acute{b} - 1)q_i + 2\acute{b}\omega_0]\}$$

$$- \frac{1}{2(T_m - 1)}e^{-q_r \ln \gamma}\{[(2\omega_0 - q_i)\beta_0 + 2\omega_0(1 - q_r)]\cos(q_i \ln \gamma)$$

$$- [(1 - q_r)\beta_0 - 2\omega_0(2\omega_0 - q_i)]\sin(q_i \ln \gamma)\},$$

[103]

in which γ, q_r and q_i are defined by

$$\gamma = \frac{T_b^0 - 1}{T_m - 1}, \quad \sqrt{1 + 4(i\omega_0 + k^2)} \equiv q_r + iq_i,$$ [104]

or, equivalently,

$$\begin{Bmatrix} q_r \\ q_i \end{Bmatrix} = \frac{\sqrt{2}}{2}\sqrt{\sqrt{(1 + 4k^2)^2 + 16\omega_0^2} \pm (1 + 4k^2)},$$ [105]

where the principal root has been taken in the definition [104].

It is readily seen that, for $\gamma_s^* = 0$, the solution for the perturbation coefficient β_1 is proportional to the factor $\epsilon_s(1 - \epsilon_s)^{-1}$, and that it consists of the sum of two contributions $\hat{\beta}_r$ and $\hat{l}^*\hat{\beta}_l$ that represent variations in the location of the neutral stability boundary that are due to non-zero density and thermal conductivity ratios $\hat{r}$ and $\hat{l}$, respectively. That is,

$$\beta_1 = \frac{\epsilon_s}{1 - \epsilon_s}[\hat{\beta}_r + \hat{\beta}_l \hat{l}^*] \quad (\gamma_s^* = 0),$$ [106]

where plots of $\hat{\beta}_r(k; \acute{b})$ and $\hat{\beta}_l(k; \acute{b})$ are displayed in figure 3(a)–(d). Positive values of these coefficients represent an upward, stabilizing shift in the neutral stability boundary from its leading-order position shown in figure 2, while negative values represent a downward, destabilizing shift. The magnitude of these perturbations in the stability boundary, whether positive or negative, is seen from [106] to increase with increasing values of the porosity ϵ_s. In addition, there is a wavenumber dependence for each effect, with non-zero values of $\hat{l}$ being destabilizing for small
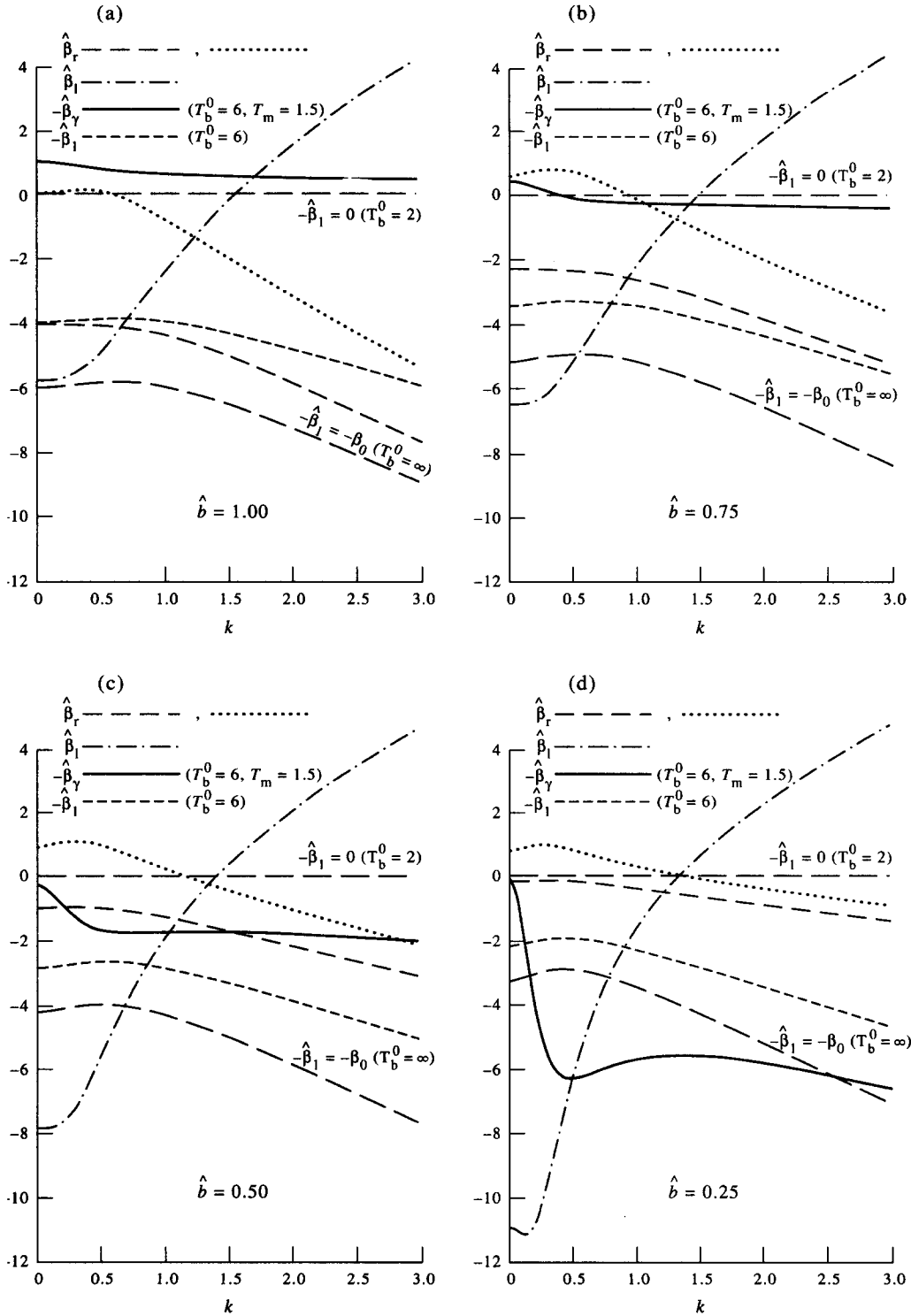
Figure 3(a)–(d). Neutral stability perturbation coefficients as a function of wavenumber for (a) $\hat{b} = 1.0$, (b) $\hat{b} = 0.75$, (c) $\hat{b} = 0.5$ and (d) $\hat{b} = 0.25$. The chain–dash curve for $\hat{\beta}_r(k; \hat{b})$ in each figure corresponds to the thermally expansive, quasi-steady gas-phase theory presented here. The dotted curve for this coefficient, which is generally located above the chain–dash curve, denotes the corresponding result for the case of a constant-density, but fully non-steady, gas phase (Margolis & Williams 1995b).

wavenumbers and stabilizing for large wavenumbers. The effect of non-zero values of $\hat{r}$, while generally destabilizing, exhibits the opposite trend (increasing destabilization for increasing wavenumbers), consistent with the physical expectation that the gas-to-solid/liquid thermal diffusivity ratio of the gas to that of the condensed phases, which is equal to $\hat{l}/\hat{b}\hat{r}$, should play a key role in determining the stabilizing or destabilizing influence of the gas phase.

The curves for $\hat{\beta}_i$ are seen in figure 3(a)–(d) to be unchanged from those in Margolis & Williams (1995b), whereas those corresponding to $\hat{\beta}_r$ [the chain–dash curves in figure 3(a)–(d)] generally lie below the corresponding dotted curves that are obtained when thermal expansion of the gas is neglected and full non-steadiness is allowed, particularly for low wavenumbers (the two corresponding expressions for $\hat{\beta}_r$ approach the same common asymptote in the limit of large k). Thus, both approximations (ideal quasi-steady gas phase and constant-density, but fully non-steady, gas phase) predict the same qualitative trend with respect to thermal diffusivity. In particular, the effect of larger gas-phase thermal diffusivities is stabilizing for short perturbation wavelengths, since the external transverse diffusive effect provided by the gas phase naturally tends to dampen such disturbances, which are produced by the diffusional/thermal instability associated with combustion of the condensed material. This effect diminishes and eventually reverses as the transverse disturbance wavelength increases and the effects of gas-phase diffusion in the negative normal direction to the perturbed front (toward the unburned material) become more significant than those associated with transverse diffusion. In connection with the latter, we note the following qualitative feedback mechanism, based on the "excess enthalpy" theory of pulsating flames. When the temperature at the front is perturbed in a positive sense, the reaction rate increases and the front accelerates. In the absence of gas-phase diffusion, the steepening temperature gradient ahead of the front then increases the heat flux away from the reaction zone, resulting in a deceleration of the front. As the reaction partially extinguishes, the process reverses so as to complete one cycle in the pulsating motion of the front. When gas-phase diffusion is present and the temperature at the front is perturbed in a positive sense, diffusion of heat through the gas from the reaction front towards the porous preheat region also increases the local propagation velocity over what it would be if the only gas-phase transport process were that of convection (towards the burned gas). Thus, the effects of an enhanced reaction rate and those associated with gas-phase diffusion are positively coupled, thereby accounting for the destabilization mechanism as the stabilizing effect of transverse gas-phase diffusion becomes small.

With respect to diffusional/thermal instability, the differences between a thermally expansive, quasi-steady gas phase relative to a constant density, fully nonsteady gas phase are confined to the downward (destabilizing) shift in the curve $\hat{\beta}_r(k)$ of the former relative to the latter, since the remaining curves are identical. In particular, there is now no stabilizing effect for small wavenumbers associated with non-zero values of $\hat{r}$ and $\hat{b}$ of order unity [compare the curves for $\hat{\beta}_r$ in figure 3(a)–(d)]. However, we note that although the allowance for gas-phase thermal expansion is more realistic than the constant-density approximation for this phase, it seems plausible that the assumption of an instantaneously responsive (i.e. quasi-steady) response for the gas may result in some overstatement of this destabilizing effect. Indeed, if a quasi-steady approximation were also adopted for the previous constant-density model, the two sets of curves for $\hat{\beta}_r$ would become identical. This follows from the fact that differences between the two asymptotic models are confined to additional time-derivative terms for the fully non-steady case, as can be seen from a comparison of [55] in the present work with the corresponding result [69] in Margolis & Williams (1995b). On the other hand, in assessing the role of gas-phase thermal expansion, a reasonable comparison of the two models would likely involve different values of $\hat{r}$ (smaller values for the constant-density case) to compensate for the fact that $\hat{r}$ refers to the upstream gas density in the thermally expansive model, which is larger than some average value appropriate for a constant-density theory. Thus, since smaller values of $\hat{r}$ would correspond to a smaller destabilizing shift in the neutral stability boundary according to [93] and [106], we conclude that the additional destabilizing effect predicted by the quasi-steady, thermally expansive model (see figure 2) is associated with both thermal expansion and the quasi-steadiness of the gas phase.

To complete our discussion, we now consider briefly the remaining curves in figure 3(a)–(d). In particular, for non-zero values of γ_s^*, there is a third component $\gamma_s^*\hat{\beta}_\gamma$ to the solution of β_l that is independent of ϵ_s and, assuming an endothermic heat of melting $(\gamma_s^* < 0)$, corresponds to the

effect of increasing the amount of heat released in the reaction zone by the amount of heat absorbed by the liquid that accompanies the phase change in the preheat region. That is,

$$\beta_1 = \frac{\epsilon_s}{1 - \epsilon_s}[\hat{\beta}_r + \hat{\beta}_l \hat{l}^*] + \hat{\beta}_\gamma \gamma_s^*, \qquad [107]$$

where the influence of the first two terms is unchanged from above. The effect of melting can be stabilizing or destabilizing, and has been discussed previously. Endothermic melting tends to be destabilizing, especially for smaller, more typical values of b and larger wavenumbers. This trend may be attributed to the fact that the release of the heat of melting by the liquid-to-gas reaction serves to enhance the heat release in the highly temperature-sensitive reaction zone, and for $\hat{b} < 1$, a greater proportion of this energy is absorbed by the reactive condensed phase relative to that absorbed by the non-reactive gas. A similar destabilizing result was predicted for low-temperature melting in gasless systems (Aldushin *et al.* 1987), although this effect diminishes and then reverses as the melting temperature increases such that melting occurs within the reaction zone itself (Margolis 1991). Here, too, the effect of increasing T_m (while keeping T_b^0 and all other parameters fixed) is found to be stabilizing, particularly for small wavenumber disturbances (Margolis & Williams 1995b).

The final $O(\hat{r})$ effect to be accounted for is due to the change in the stability parameter β itself that accompanies any variation in the density ratio $\hat{r}$. Although we have thus far adhered to a conventional definition of the Zel'dovich number as defined by [38], this parameter itself varies with $\hat{r}$ through changes in the burned temperature T_b. In particular, for small values of $\hat{r}$, T_b decreases as $\hat{r}$ increases according to [86], thereby increasing the effective activation energy. Defining a modified Zel'dovich number β^0 that does not vary with $\hat{r}$ according to

$$\beta^0 = (1 - T_b^0)N^0, \quad N^0 \equiv \frac{\tilde{E}_1}{\tilde{R}^\circ T_b^0}, \qquad [108]$$

where T_b^0 is the leading-order burned temperature defined in [86], we calculate an additional correction $-\epsilon_s(1 - \epsilon_s)^{-1}\hat{\beta}_1 \hat{r}$ in the position of the neutral stability boundary with respect to the new parameter β^0, where $\hat{\beta}_1 = (1 - 2/T_b^0)\hat{\beta}_0$ is shown in figure 3(a)–(d) for several values of T_b^0, and $\beta_0(k)$ is the leading-order neutral stability boundary determined from [90]. That is, analogous to [93] and [107],

$$\beta^0 \sim \beta_0 + \left[\frac{\epsilon_s}{1 - \epsilon_s}\left(\hat{\beta}_r + \hat{\beta}_l \hat{l}^* - \frac{T_b^0 - 2}{T_b^0}\beta_0\right) + \hat{\beta}_\gamma \gamma_s^*\right]\hat{r} + \cdots, \qquad [109]$$

where $\hat{\beta}_r(k)$, $\hat{\beta}_l(k)$ and $\hat{\beta}_\gamma(k)$ are the same coefficients as those exhibited in figure 3(a)–(d). The above two-term approximation of β^0 is shown in figure 2 (chain–dash curves) for the same values of $\hat{b}$ as the leading-order approximation β_0 for typical values of the remaining parameters. Also shown in that figure are the corresponding (chain–dot) curves for the case of constant gas-phase density, which, while still indicating an overall destabilizing effect due to gas-phase influences, nonetheless lie above the modified stability boundaries that are obtained when thermal expansion of the gas is taken into account. From [109], it is clear that since the linearized correction to the leading-order result, due to non-zero values of the density and thermal conductivity ratios $\hat{r}$ and $\hat{l}$, is proportional to $\epsilon_s(1 - \epsilon_s)^{-1}$, whereas the coefficient $\hat{\beta}_\gamma$ is independent of ϵ_s (cf. [95], [100] and [103]), the overall effect of an increase in porosity is destabilizing with respect to steady, planar deflagration and that this effect is enhanced by gas-phase thermal expansion.

9. SUMMARY

The present analysis has extended the multiphase-flow theory developed in several previous works for the deflagration of porous energetic materials, such as degraded nitramine propellants, that undergo exothermic reactions in a liquid layer to produce gaseous products. The focus in this study, was, as in Margolis & Williams (1995b), on the investigation of the effects of non-zero porosity on the stability of steady, planar deflagration. This was facilitated by the derivation of an appropriate asymptotic model, valid in the limit of large overall activation energies, for the general case of non-steady, multidimensional propagation in an unconfined material. In the present

work this derivation proceeded under the assumption of a thermally expansive, quasi-steady gas phase, in contrast to the constant-density, fully non-steady gas phase that was assumed previously in Margolis & Williams (1995b). A basic solution corresponding to a steady, planar deflagration was then obtained explicitly, thereby allowing a linear stability analysis of this solution to be carried out in a standard fashion. It was determined, as in previous studies, that a pulsating stability boundary exists in the plane of activation energy and disturbance wavenumber, similar to that obtained in strictly condensed combustion (combustion synthesis) and in non-porous solid-propellant combustion. The neutral stability boundary was shown to be especially accessible for realistic parameter values that furthermore permit the effects of porosity on the location of this stability boundary to be handled in a perturbative fashion. Specifically, in the realistic limit of small gas-to-solid/liquid density and thermal conductivity ratios, it was shown that shifts in the stability boundary were proportional to $\epsilon_s(1 - \epsilon_s)^{-1}$. Positive (stabilizing) shifts were then shown to be realized for perturbations corresponding to sufficiently small transverse wavelengths owing to the smoothing effects of gas-phase thermal diffusion on what is essentially a condensed-phase instability. However, this transverse smoothing effect was shown to diminish with decreasing disturbance wavenumbers such that negative (destabilizing) shifts, associated with gas-phase diffusion normal to the reaction front, occur for sufficiently large transverse wavelengths. In addition, the lowering of the burned temperature as the porosity increases was shown to be destabilizing as well, since it serves to increase the effective activation energy. The effect of thermal expansion was shown to result in a destabilizing shift in the neutral stability boundary relative to the previous constant-density analysis, although it was speculated that the assumption of gas-phase quasi-steadiness may overstate the true effect.

REFERENCES

Aldushin, A. P. 1990 Heat transfer and convection combustion regimes of porous systems with filtration of heat carrier. *Combust. Explos. Shock Waves* **26**, 180–187.

Aldushin, A. P., Vol'pert, V. A. & Filipenko, V. P. 1987 Effect of reagent melting on combustion stability for gasless systems. *Combust. Explos. Shock Waves* **23**, 408–414.

Aldushin, A. P. & Zeinenko, K. I. 1991 Combustion of pyrotechnic mixtures with heat transfer from gaseous reaction products. *Combust Explos. Shock Waves* **27**, 700–703.

Baer, M. R. & Nunziato, J. W. 1986 A two-phase mixture theory for the deflagration-to-detonation transition (DDT) in reactive granular materials. *Int. J. Multiphase Flow* **12**, 861–889.

De Luca, L. 1992 Theory of nonsteady burning and combustion of solid propellants by flame models. In *Nonsteady Burning and Combustion Stability of Solid Propellants* (Edited by De Luca, L., Price, E. W. & Summerfield, M.). *Prog. Astronaut. Aeronaut.* **143**, 519–600.

De Luca, L., Di Silvestro, R. & Cozzi, F. 1995 Intrinsic combustion instability of solid energetic materials. *J. Propulsion Power* **11**, 804–815.

Dension, M. R. & Baum, E. 1961 A simplified model of unstable burning in solid propellants. *ARS J.* **31**, 1112–1122.

Li, S. C., Williams, F. A. & Margolis, S. B. 1990 Effects of two-phase flow in a model for nitramine deflagration. *Combust. Flame* **80**, 329–349.

Maksimov, E. I. & Merzhanov, A. G. 1966 Theory of combustion of condensed substances. *Combust. Explos. Shock Waves* **2**, 25–31.

Margolis, S. B. 1991 The transition to nonsteady deflagration in gasless combustion. *Prog. Energy Combust. Sci.* **17**, 135–162.

Margolis, S. B. & Armstrong, R. C. 1986 Two asymptotic models for solid propellant combustion. *Combust. Sci. Technol.* **47**, 1–38.

Margolis, S. B. & Williams, F. A. 1988 Diffusional/thermal coupling and intrinsic instability of solid propellant combustion. *Combust. Sci. Technol.* **59**, 27–84.

Margolis, S. B. & Williams, F. A. 1989 Diffusional/thermal instability of a solid propellant flame. *SIAM J. Appl. Math.* **49**, 1390–1420.

Margolis, S. B. & Williams, F. A. 1990 Stability of homogeneous-solid deflagration with two-phase flow in the reaction zone. *Combust. Flame* **79**, 199–213.

Margolis, S. B. & Williams, F. A. 1995a Effects of two-phase flow on the deflagration of porous energetic materials. *J. Propulsion Power.* **11**, 759–768.

Margolis, S. B. & Williams, F. A. 1995b Influence of porosity and two-phase flow on diffusional/thermal instability of a deflagrating energetic material. *Combust. Sci. Technol.* **106**, 41–68.

Margolis, S. B., Williams, F. A. & Armstrong, R. C. 1987 Influences of two-phase flow in the deflagration of homogeneous solids. *Combust. Flame* **67**, 249–258.

Merzhanov, A. G. 1969 The theory of stable homogeneous combustion of condensed substances. *Combust. Flame* **13**, 143–156.

Mitani, T. & Williams, F. A. 1986 A model for the deflagration of nitramines. In *Twenty-first Symposium (International) on Combustion*, pp. 1965–1974.

Zanotti, C., Carretta, U., Grimaldi, C. & Colombo, G. 1992 Self-sustained oscillatory burning of solid propellants. In *Nonsteady Burning and Combustion Stability of Solid Propellants* (Edited by De Luca, L., Price, E. W. & Summerfield, M.). *Prog. Astronaut. Aeronaut.* **143**, 399–439.